Exclusive Physics with the HERMES Recoil Detector

Erik Etzelmüller on behalf of the HERMES Collaboration

workshop on

“Exploring Hadron Structure with Tagged Structure Functions“

Thomas Jefferson National Accelerator Facility, 18.01.2014

Content

- Motivation (GPDs - Generalized Parton Distributions)
- DVCS (Deeply Virtual Compton Scattering)
- The HERMES experiment and the Recoil detector
- Overview of the results
- Associated DVCS

Some milestones

1988	EMC publication triggers “spin crisis“
1995	HERMES experiment at DESY starts data taking. Mission: “spin puzzle“
1997	Ji finds a way to access the total angular momentum of a nucleon
2001	First HERMES DVCS paper published
2006	HERMES Recoil detector starts taking data

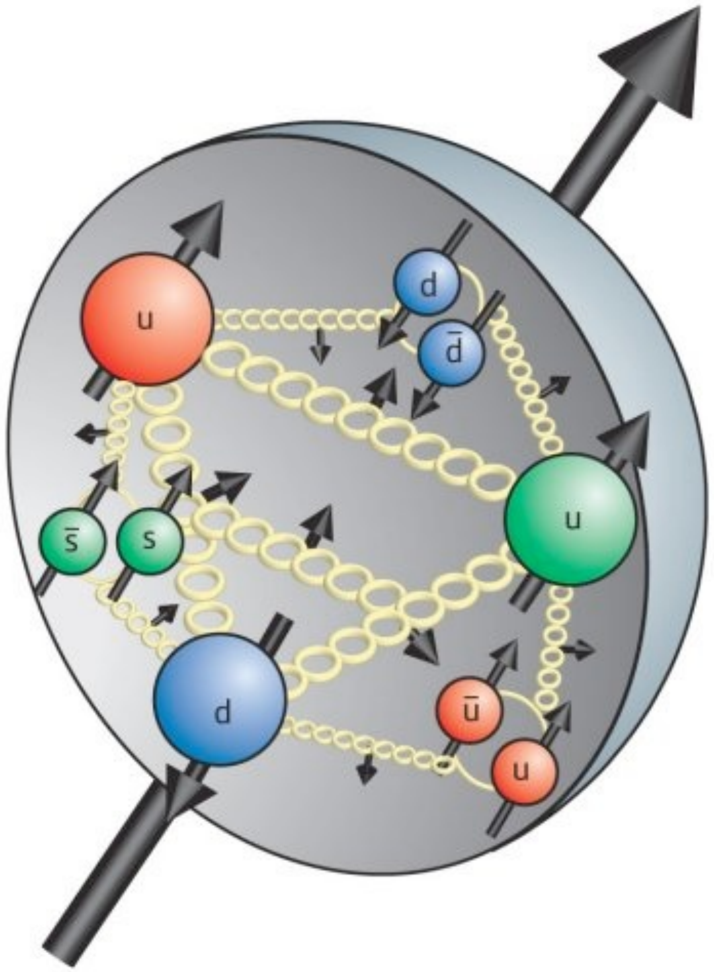

The proton spin puzzle

$$s_z = \frac{1}{2} = J_q + J_g$$

contribution from quarks lower than expected from naive quark model

$$J_q = \frac{1}{2} \cdot \Delta\Sigma + L_q$$

Ji found a way to access total angular momentum through GPDs [X. Ji, Phys. Rev. Lett. 78 (1997) 610]:

$$J_q = \frac{1}{2} \cdot \Delta\Sigma + L_q = \frac{1}{2} \int_{-1}^{1} \mathrm{d}x\, x \left[H_q(x, \xi, t=0) + E_q(x, \xi, t=0) \right]$$

GPDs

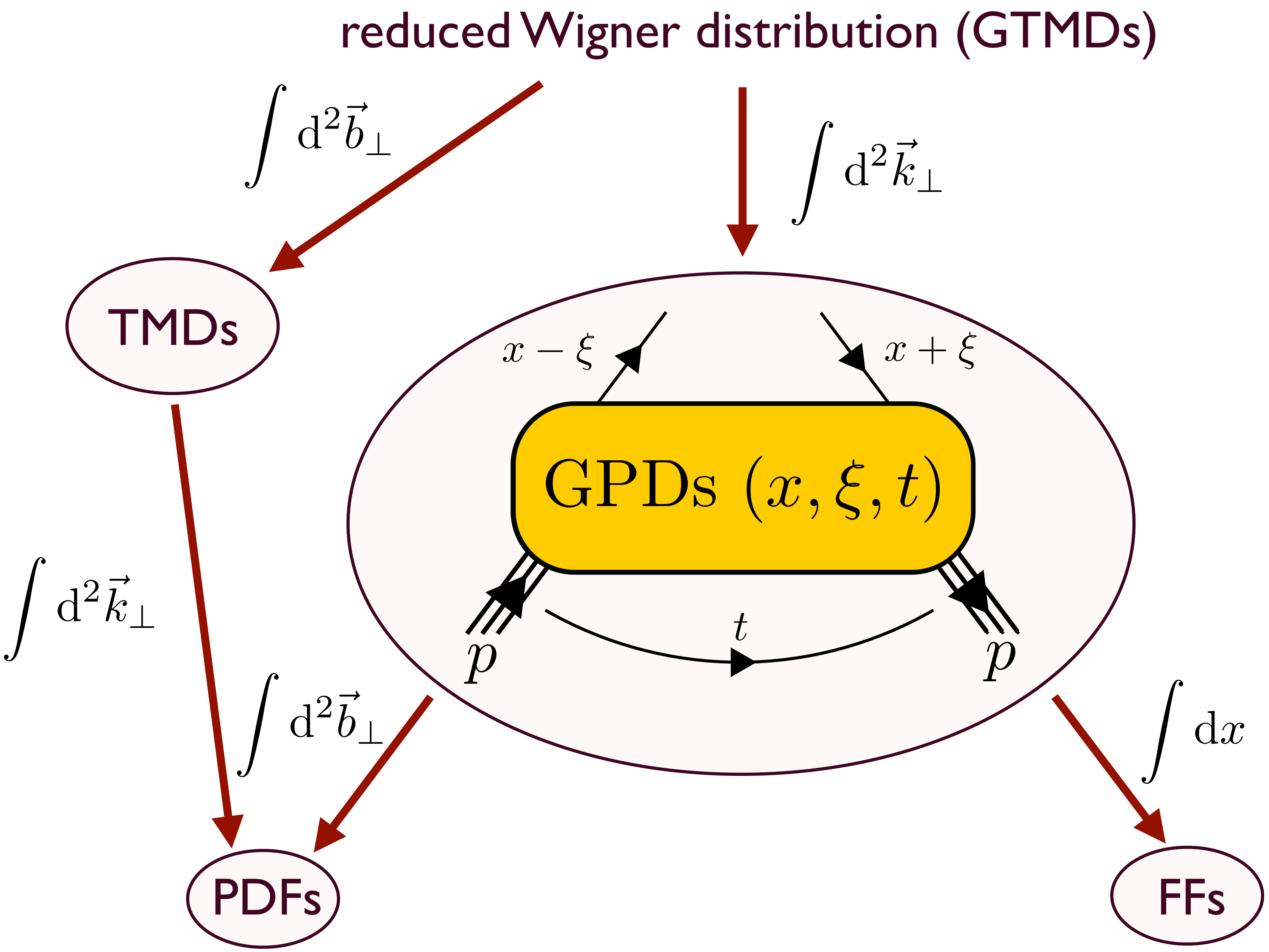
reduced Wigner distribution (GTMDs)
$\int d^2\vec{b}_\perp$
$\int d^2\vec{k}_\perp$
TMDs
$x-\xi$
$x+\xi$
GPDs (x,ξ,t)
p
t
p
$\int d^2\vec{k}_\perp$
$\int d^2\vec{b}_\perp$
$\int dx$
PDFs
FFs

GPDs

Experimentally GPDs can be accessed through measurements of hard exclusive lepton-nucleon scattering processes.

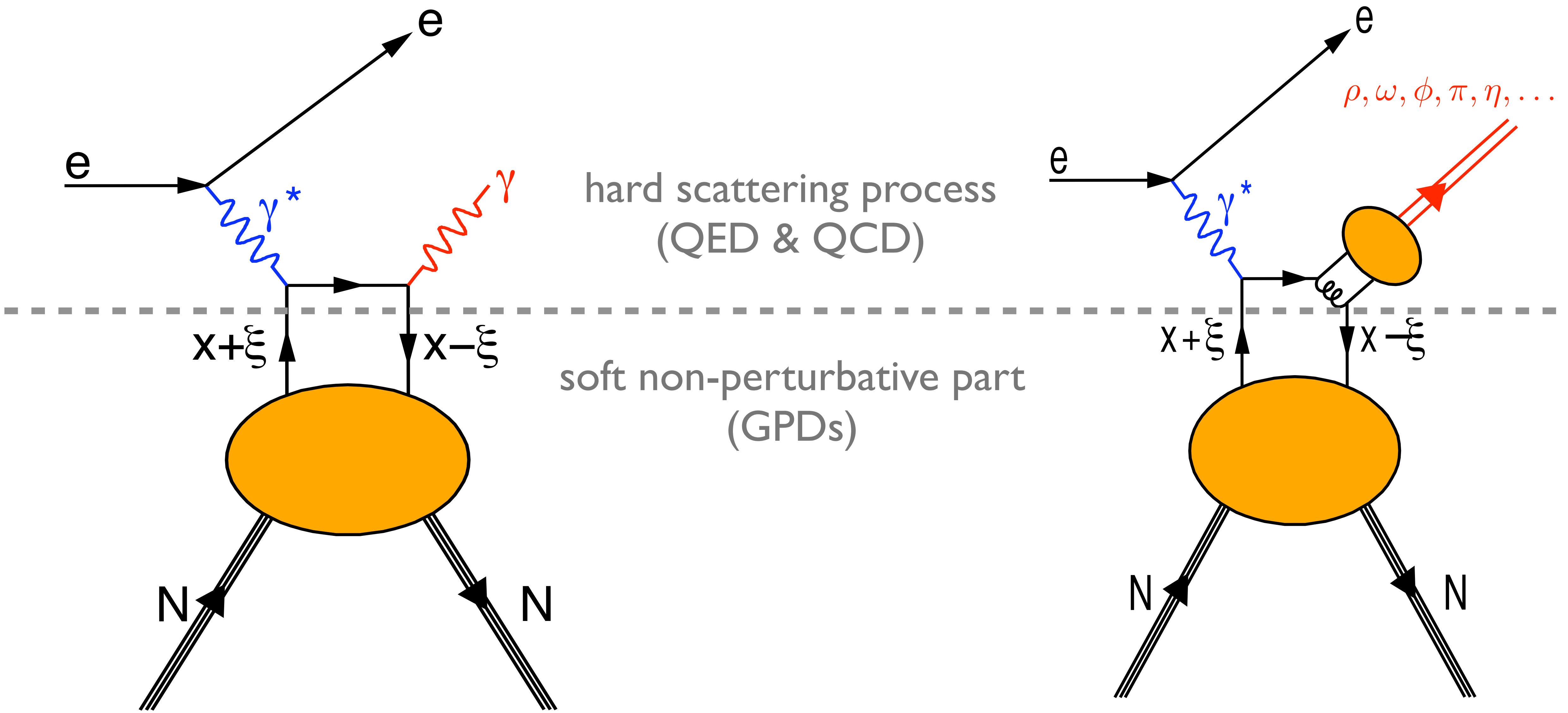

DVCS
deeply virtual Compton scattering

HEMP
hard exclusive meson production

Theoretically cleanest access to GPDs through DVCS

But: final and initial state is equal to Bethe-Heitler scattering (BH)

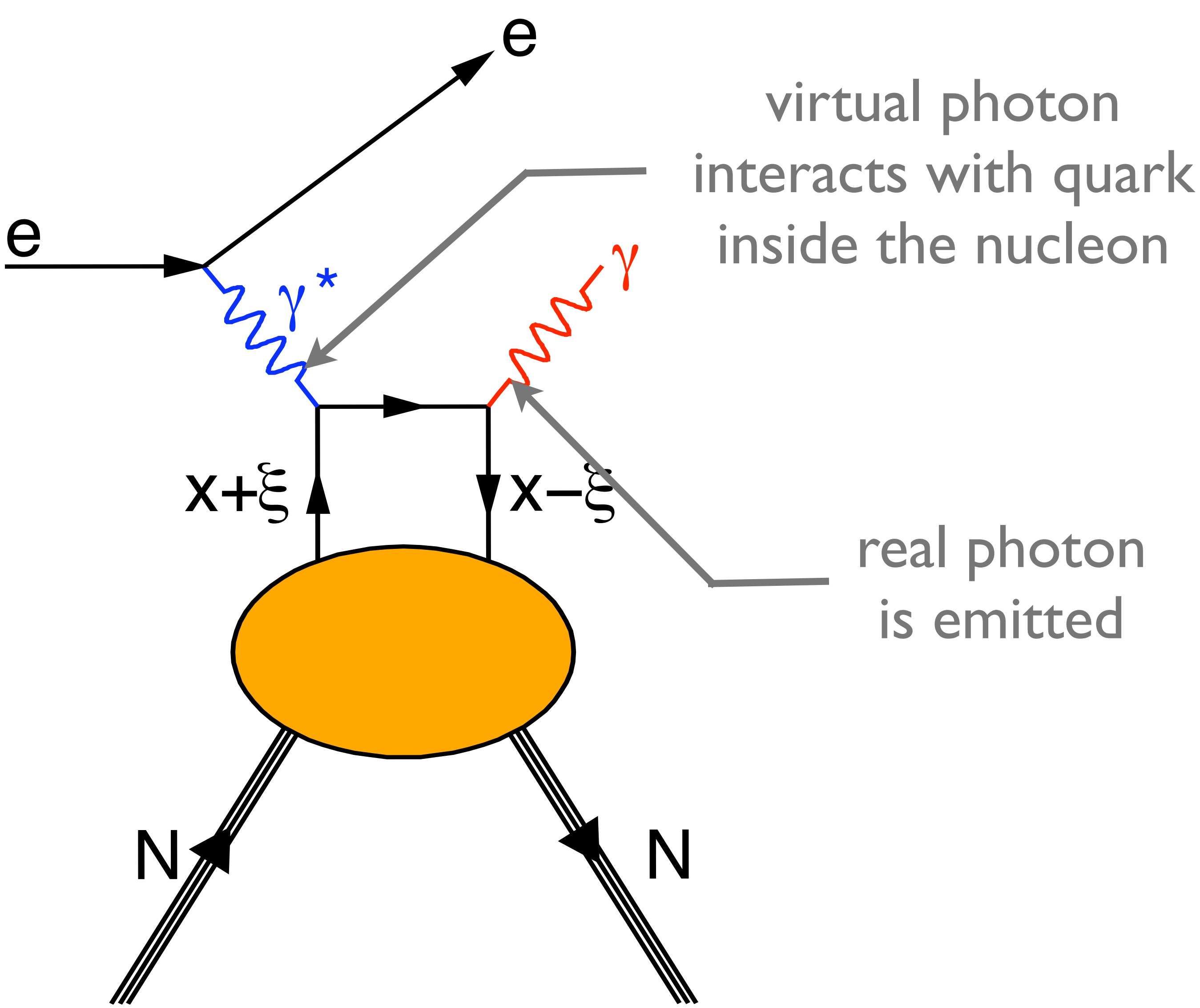

DVCS

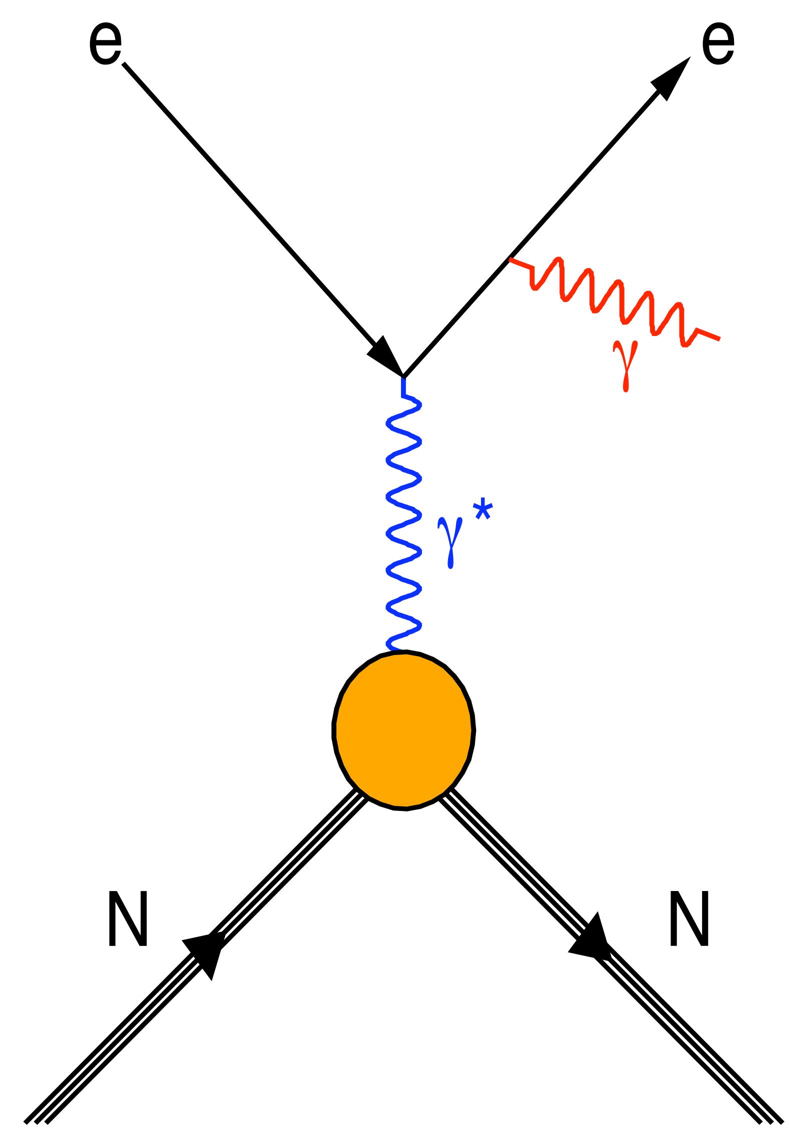

BH

$$\frac{\mathrm{d}^4\sigma}{\mathrm{d}Q^2\mathrm{d}x_B\mathrm{d}t\mathrm{d}\phi} = \frac{x_B e^6}{32(2\pi)^4 Q^4\sqrt{1+\epsilon^2}} \left|\mathcal{T}_{ep\rightarrow ep\gamma}\right|^2$$

$$\left|\mathcal{T}_{ep\rightarrow ep\gamma}\right|^2 = \left|\mathcal{T}_{BH}\right|^2 + \left|\mathcal{T}_{DVCS}\right|^2 + \mathcal{I}$$

Amplitude of Bethe-Heitler scattering is dominant at HERMES kinematics

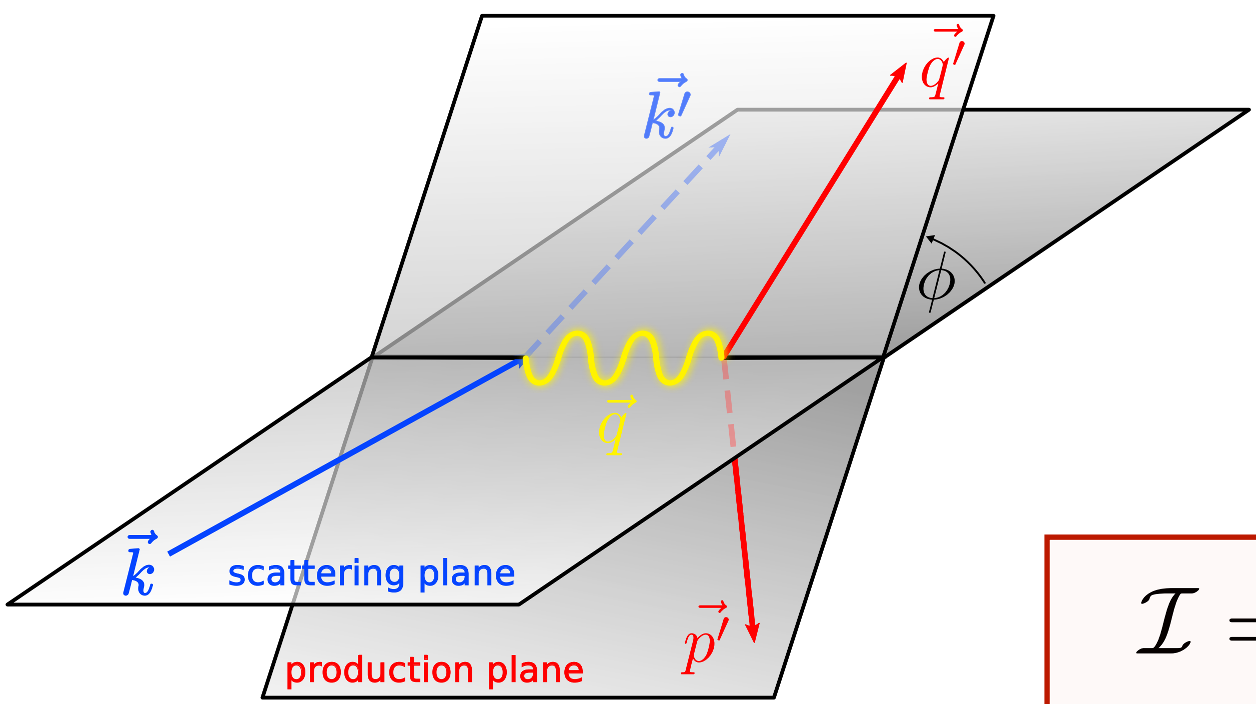

DVCS amplitude is amplified by BH in the interference term

$$\mathcal{I} = \mathcal{T}_{BH}\mathcal{T}^*_{DVCS} + \mathcal{T}_{DVCS}\mathcal{T}^*_{BH}$$

Access through the measurement of asymmetries:

$$\mathcal{A}_{\mathrm{LU}}(\phi, e_l) = \frac{\sigma_{\mathrm{LU}}(\phi, e_l, \lambda = +1) - \sigma_{\mathrm{LU}}(\phi, e_l, \lambda = -1)}{\sigma_{\mathrm{LU}}(\phi, e_l, \lambda = +1) + \sigma_{\mathrm{LU}}(\phi, e_l, \lambda = -1)}$$

$$= \frac{1}{\sigma_{\mathrm{UU}(\phi, e_l)}} \left[K_{DVCS}\, s_1^{DVCS} \sin\phi - \frac{e_l K_{\mathcal{I}}}{\mathcal{P}_1(\phi)\mathcal{P}_2(\phi)} \sum_{n=1}^{2} s_n^{\mathcal{I}} \sin(n\phi) \right]$$

longitudinally polarized beam, unpolarized target

Fourier coefficients comprise Compton-Form factors (CFFs) which are convolutions of the GPDs with the hard scattering kernel.

Example:

$$A_{\mathrm{LU}}(\phi) \sim \pm \frac{x_B}{y} \frac{s_1^{\mathcal{I}}}{c_0^{\mathrm{BH}}} \sin(\phi) \propto \Im\mathrm{m} \left\{ F_1 \mathcal{H} + \frac{x_B}{2 - x_B}(F_1 + F_2)\widetilde{\mathcal{H}} - \frac{t}{4M^2} F_2 \mathcal{E} \right\} \sin(\phi)$$

The HERMES experiment

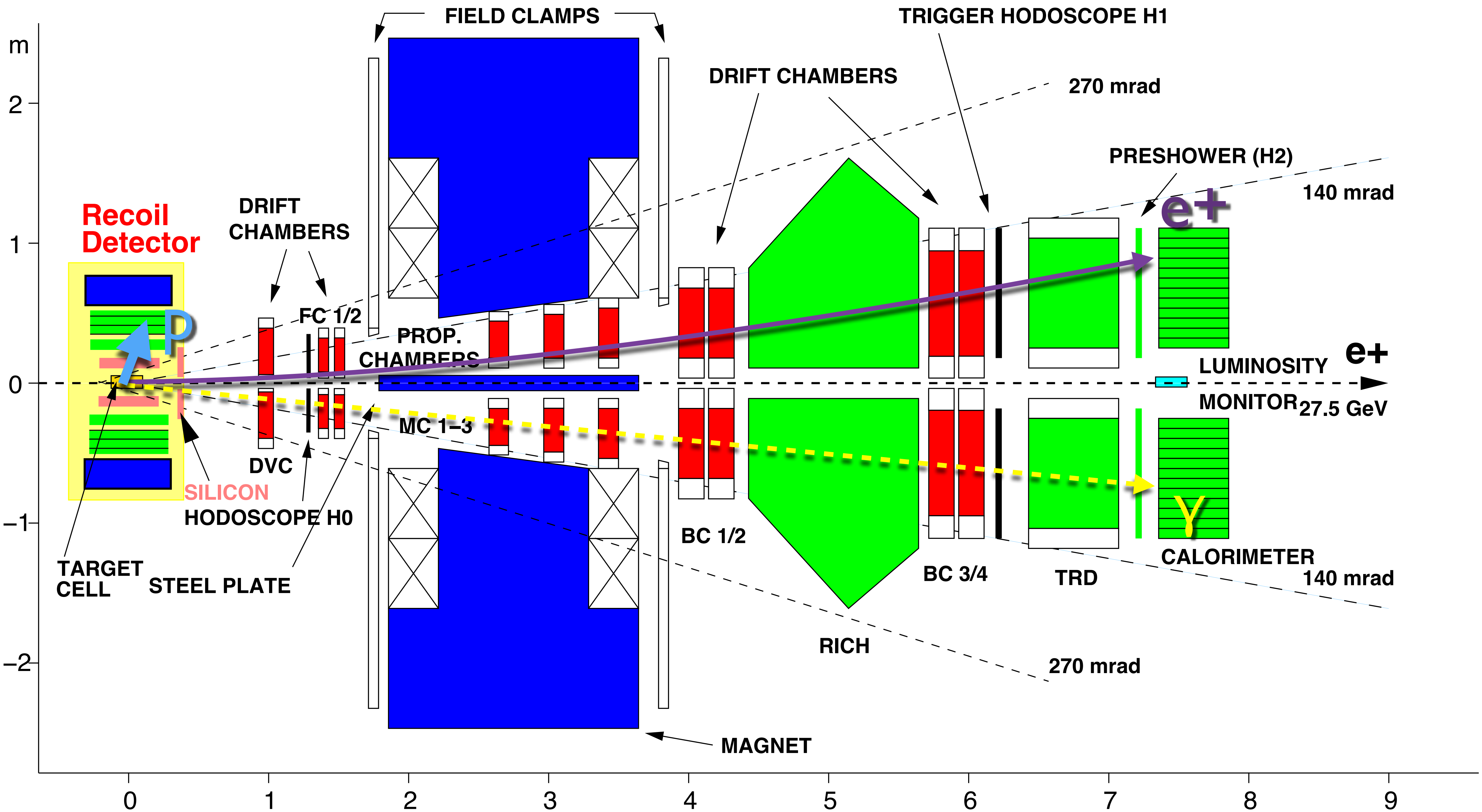

Recoil detector upgrade for 2006/2007 running

The HERMES Recoil detector

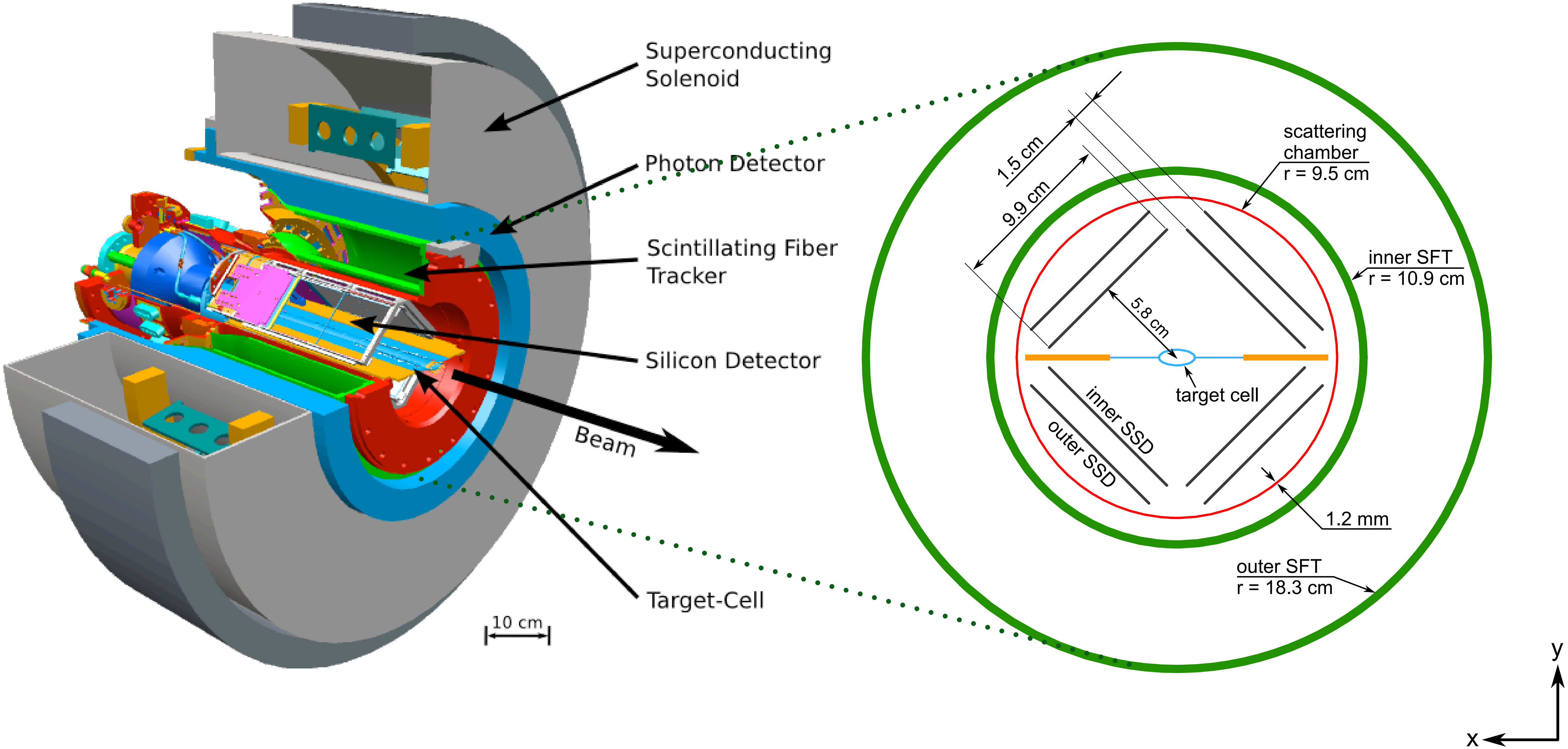

Enables the measurement of the recoiling charged particle and therefore full ep→epγ event reconstruction

The HERMES Recoil detector

Sketch of front- and backside of a silicon strip detector module (SSD)

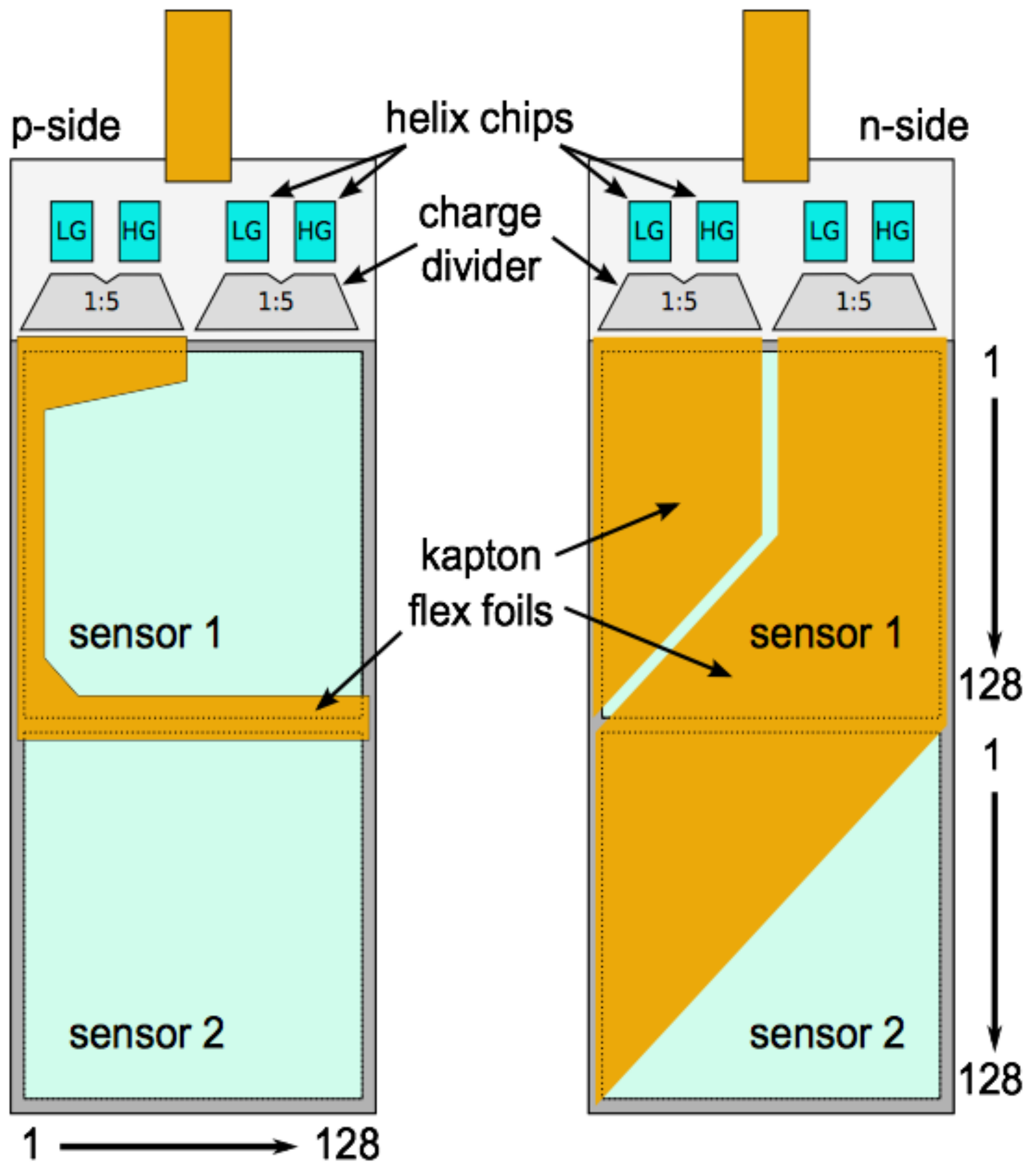

Schematic design of the scintillating fibre tracker (SFT)

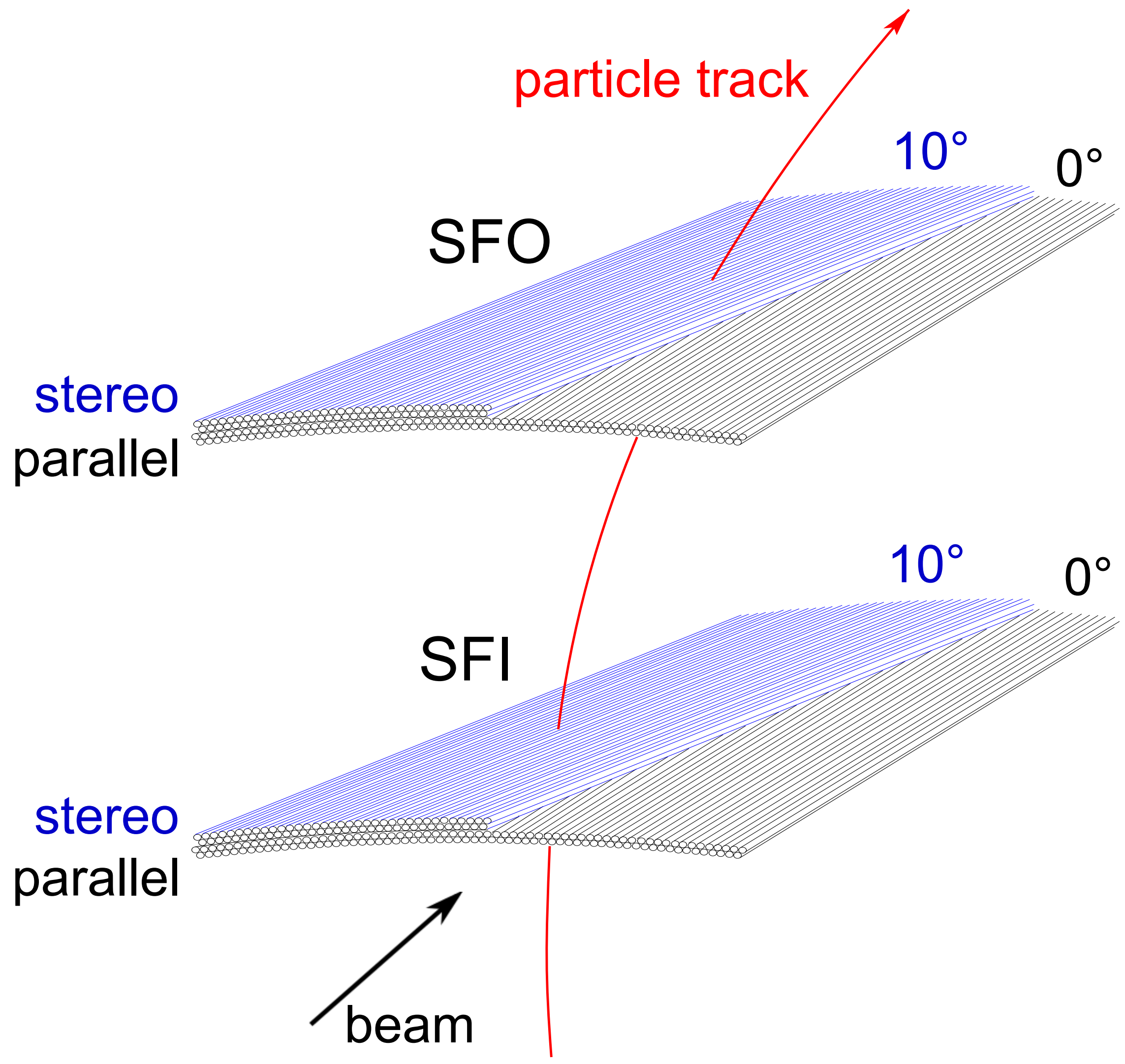

The HERMES Recoil detector

The silicon strip detector (SSD)

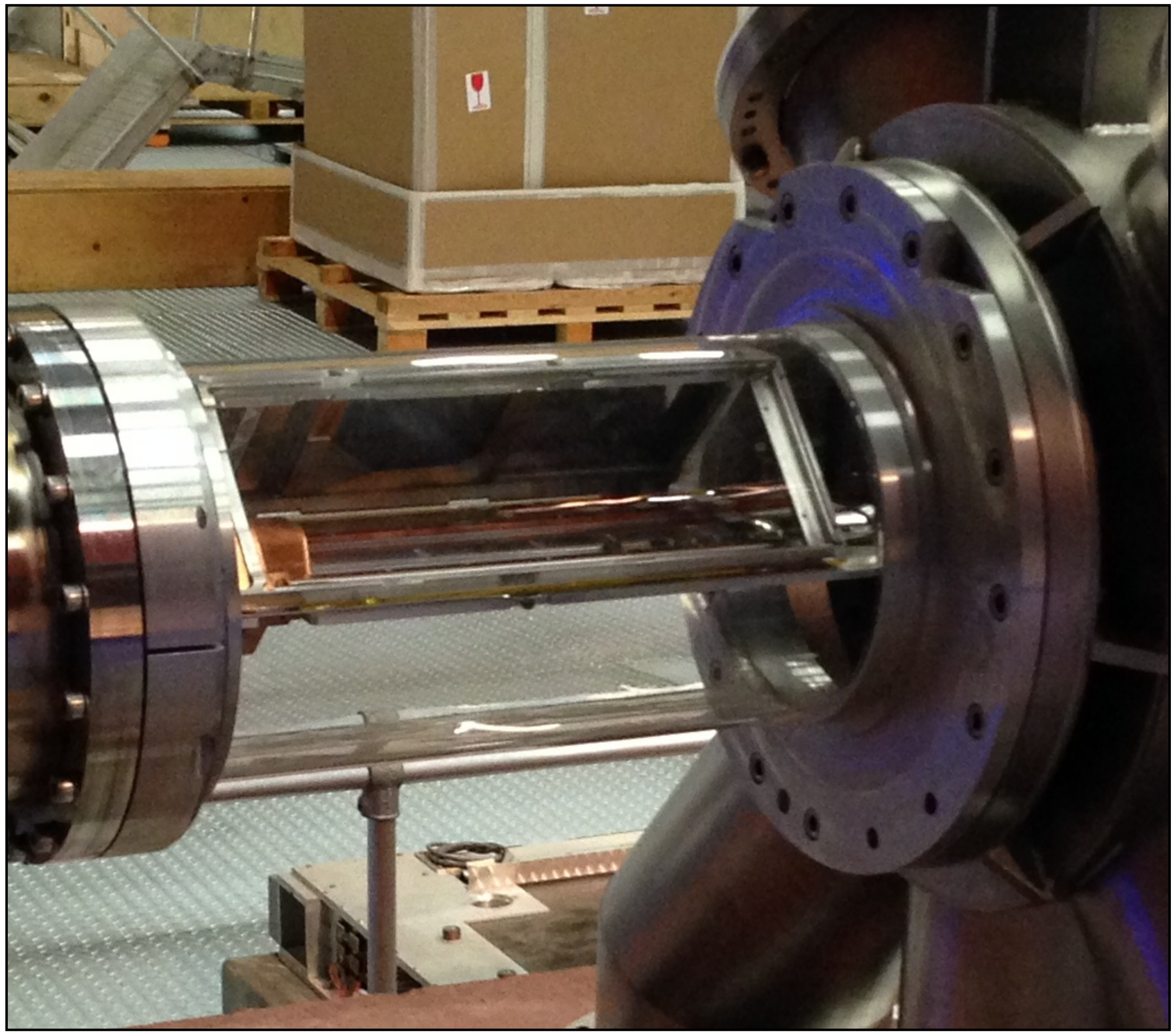

The scintillating fibre tracker (SFT)

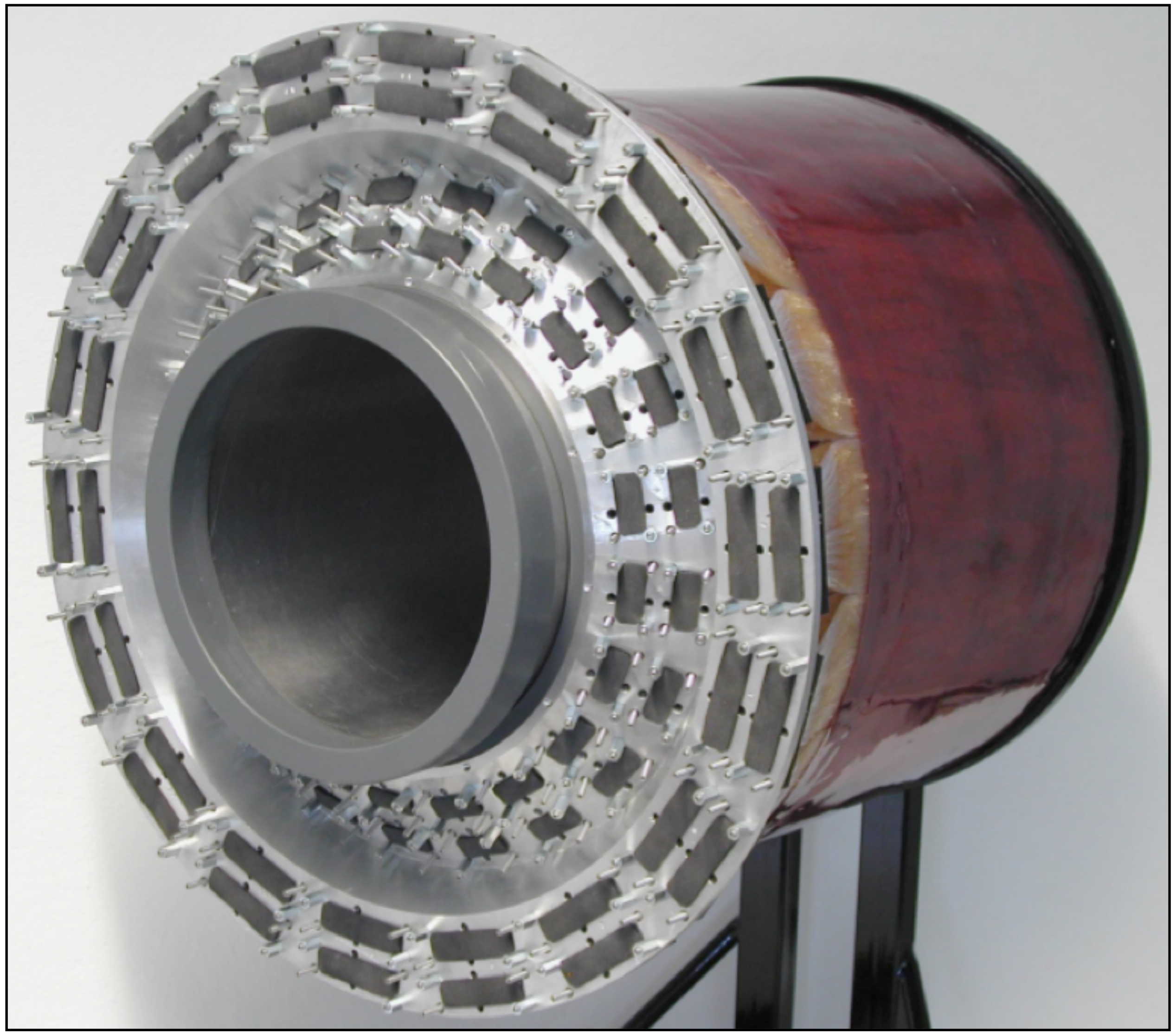

Kinematic coverage

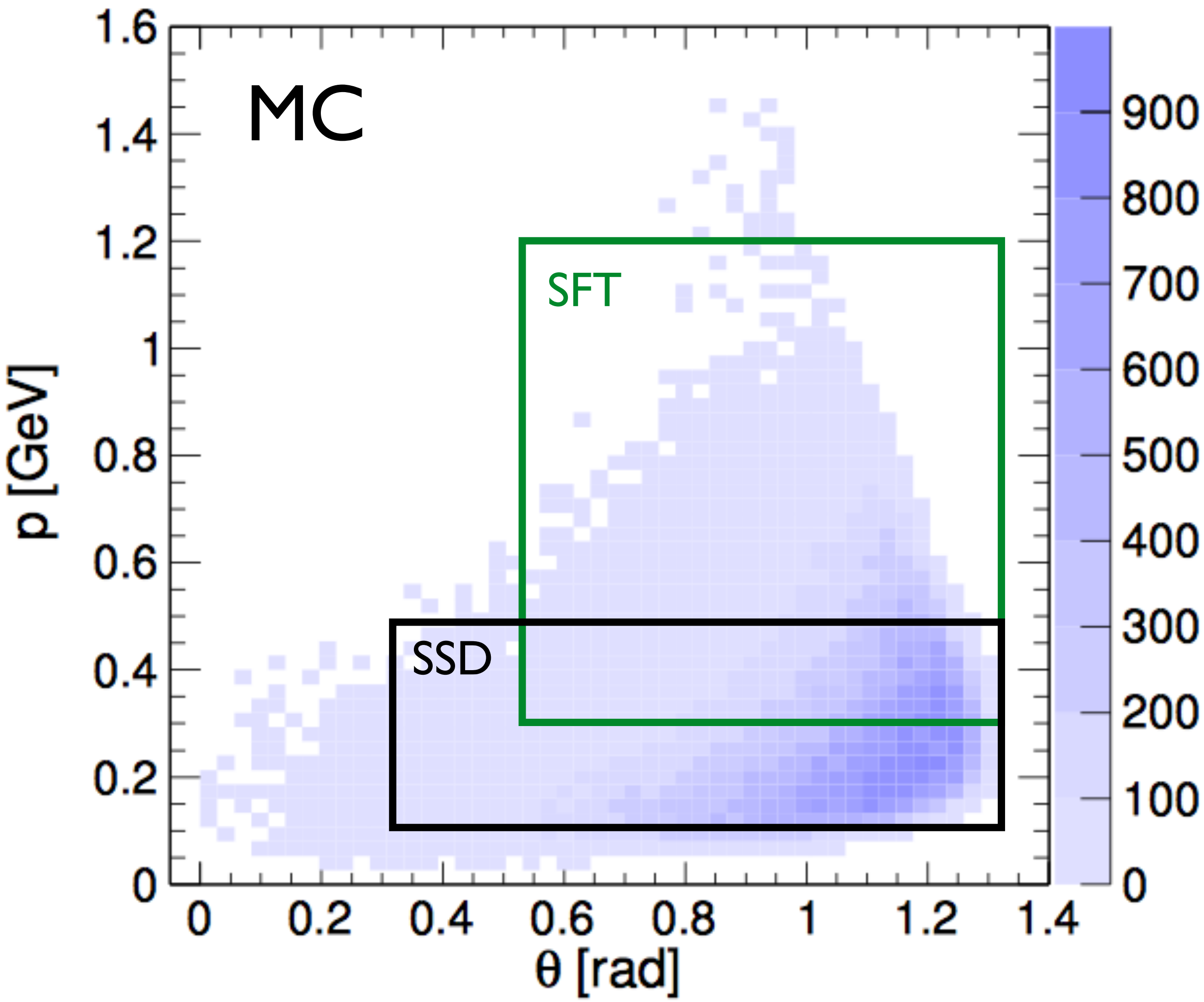

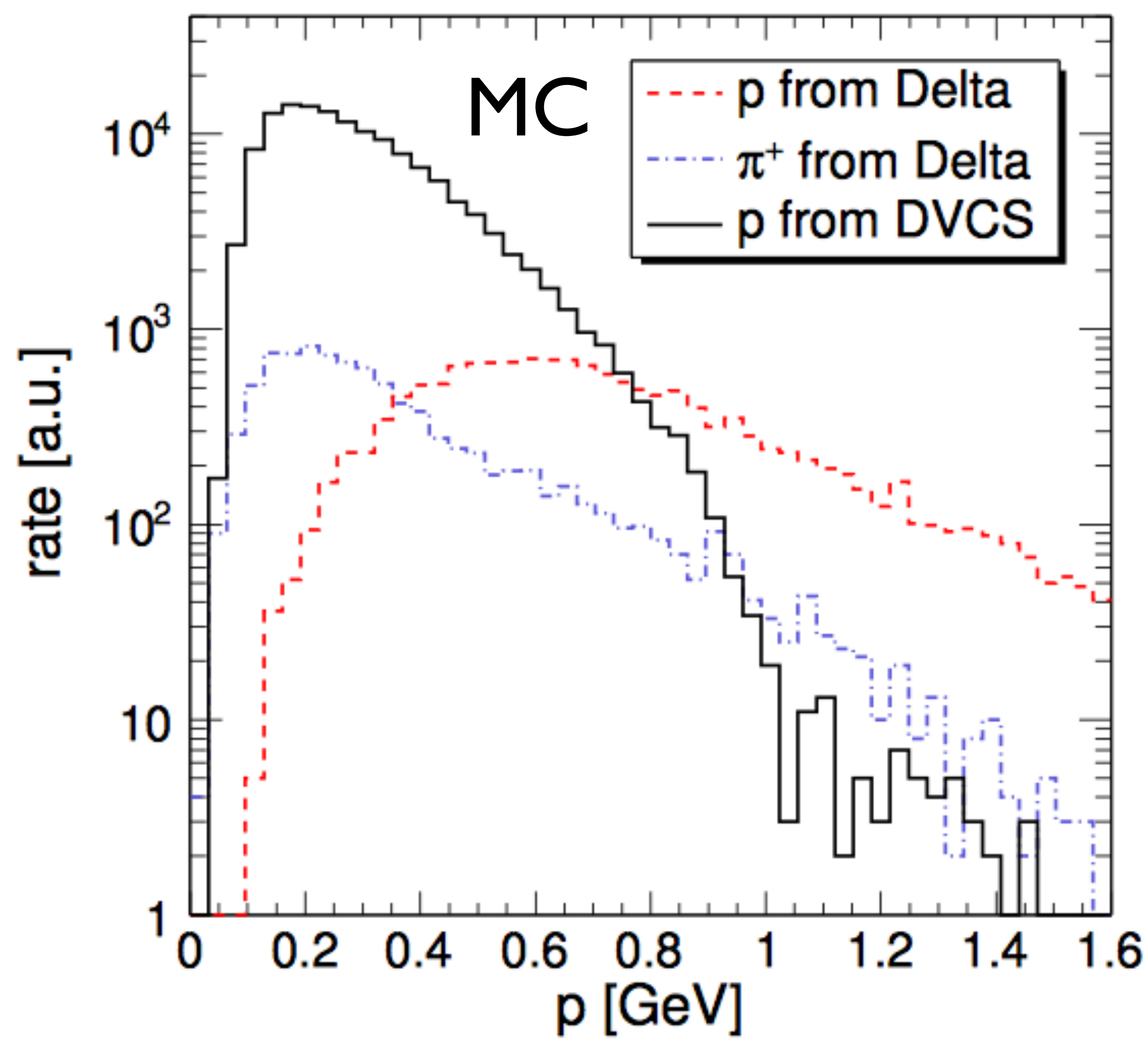

Scintillating fibre tracker (SFT) and silicon strip detector (SSD) complement each other

Improvement through the Recoil detector

forward spectrometer only | measured proton

similar background

same kinematic acceptance

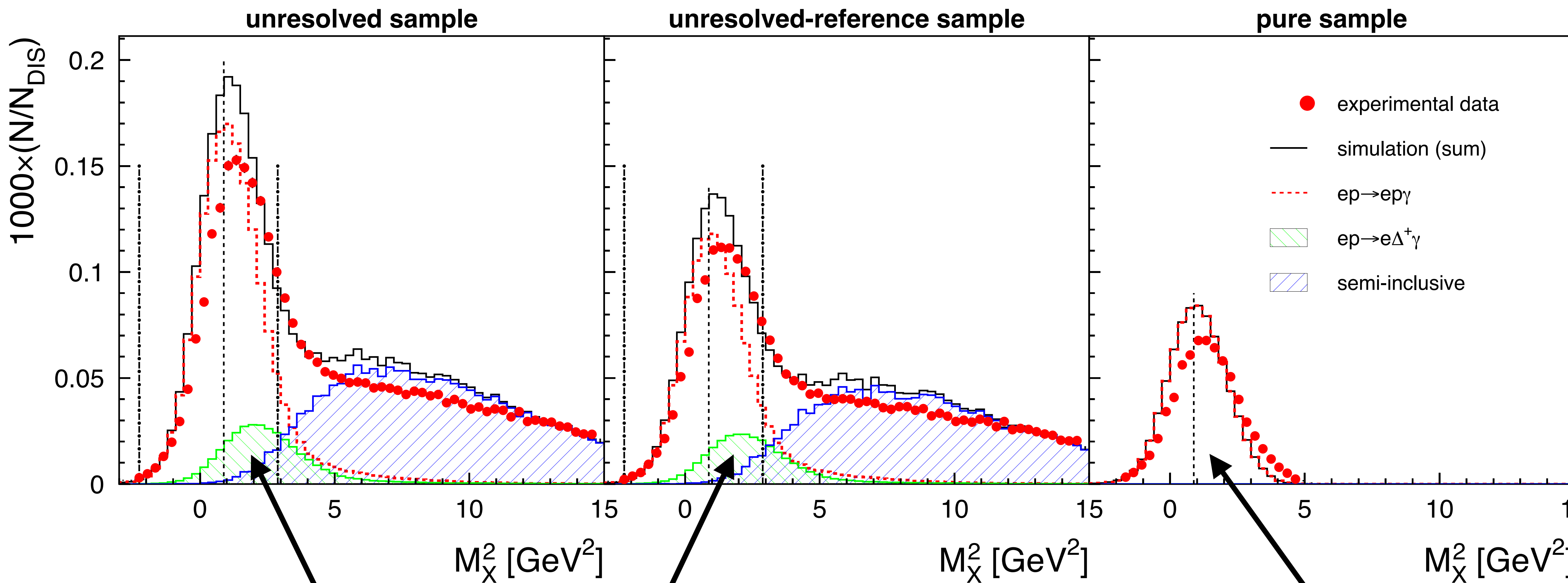

associated processes ($ep \to e\gamma\Delta^+$)

pure $ep \to e\gamma p$

Missing mass:

$$M_x^2 = (k - k' + P_0 - P_\gamma)^2 = M^2 + 2M(\nu - E_\gamma) + t$$

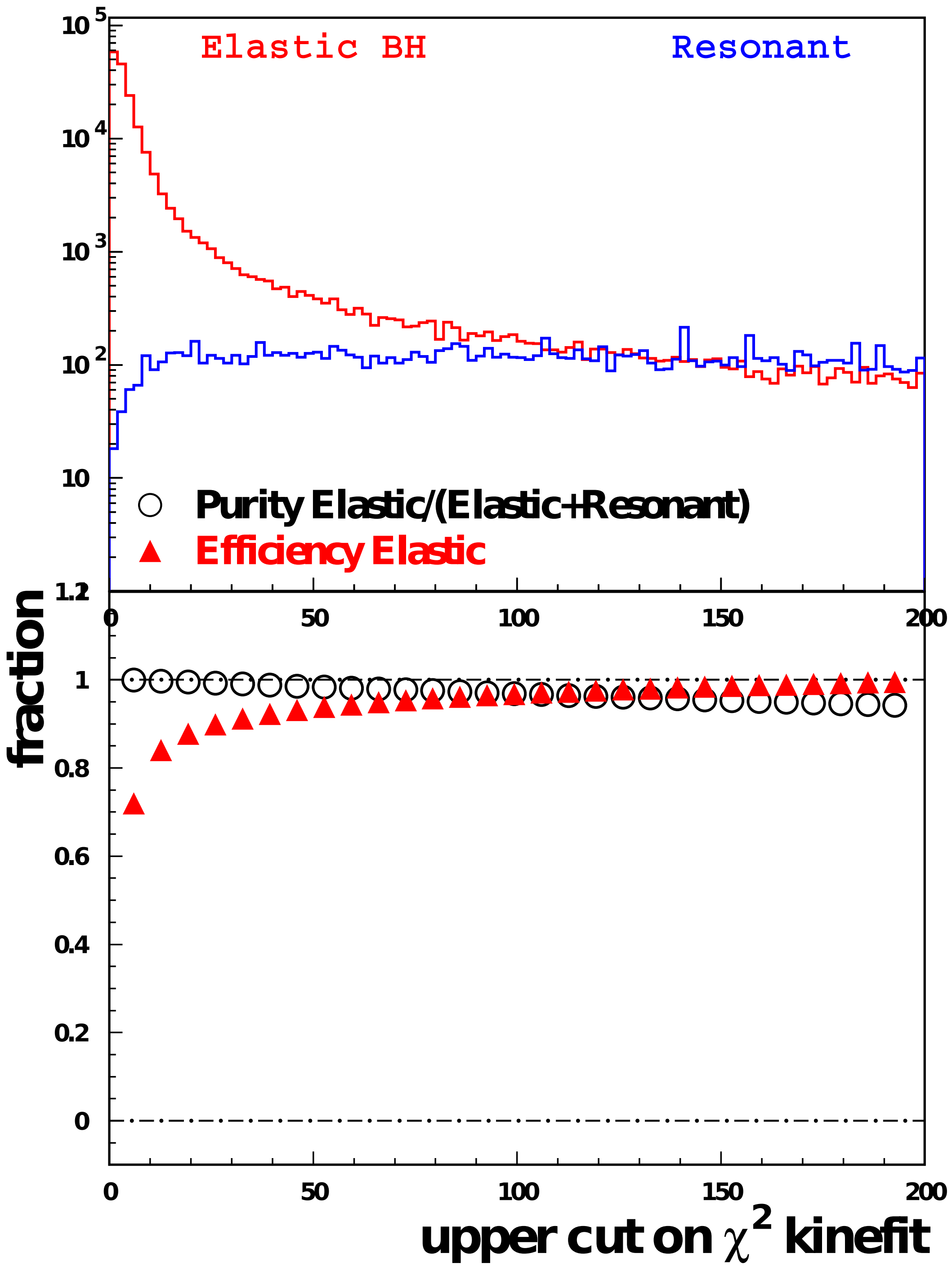

Kinematic event fitting:

$$\chi^2_{pen} = \sum_{i=1}^{9} \frac{(r_i^{fit} - r_i^{meas})^2}{\sigma_i^2} + T \cdot \sum_{j=1}^{4} \frac{\left[f_j(r_1^{fit}, \ldots, r_9^{fit}) \right]^2}{(\sigma_j^f)^2}$$

χ^2-value of interest — penalty term — constraints

- 4-momentum conservation as constraints
- lowest χ^2-value in case of multiple recoil tracks per event
- minimum of 1 % fit probability required, which corresponds to $\chi^2 < 13.7$

Beam-spin asymmetries ep→eγp

A. Airapetian et al, JHEP10 (2012) 042

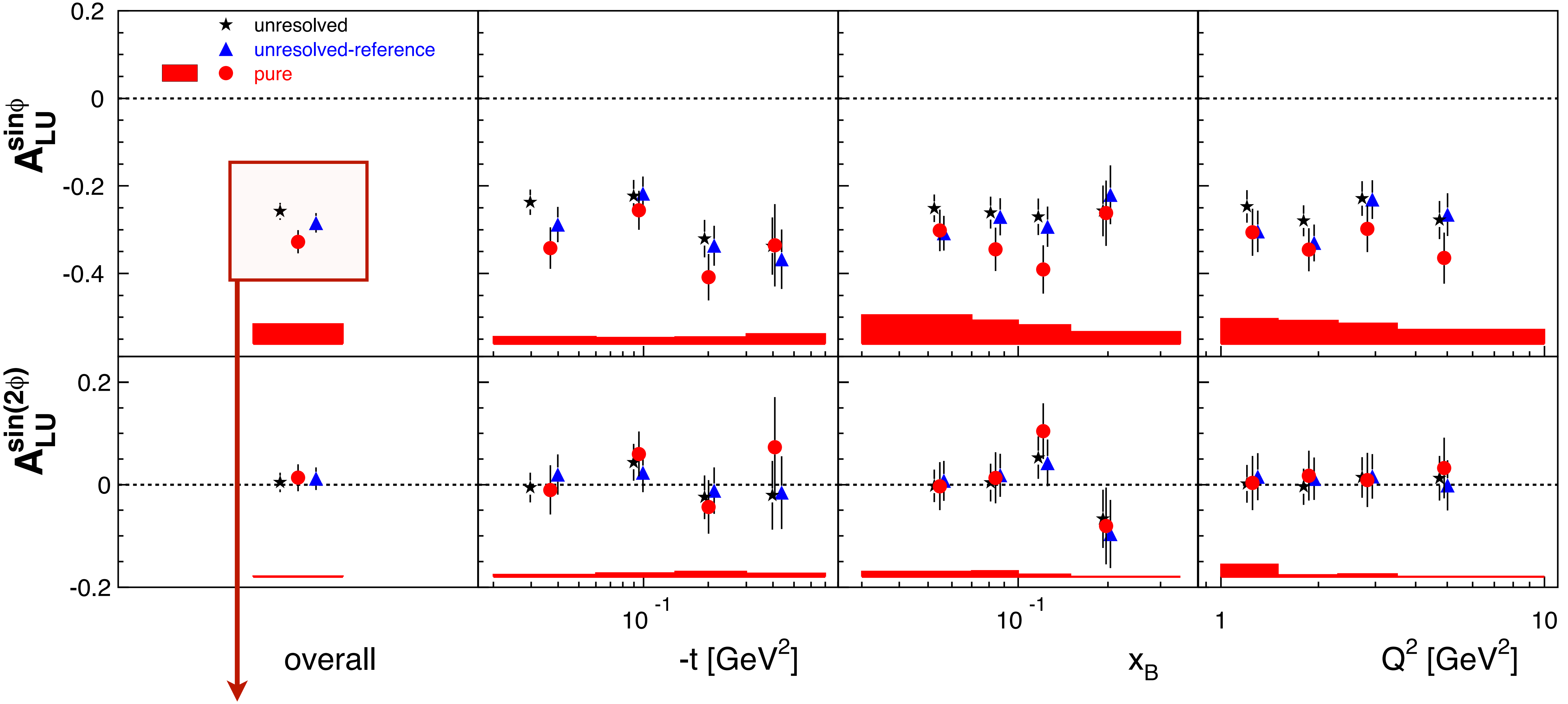

Magnitude of the leading asymmetry has increased by 0.054 ± 0.016

All sets are strongly correlated but the unresolved samples contain an average contribution of 12 -14 % of associated processes

Beam-spin asymmetries ep→eγp

P. Kroll, H. Moutarde, F. Sabatié, Eur. Phys. J. C (2013) 73:2278

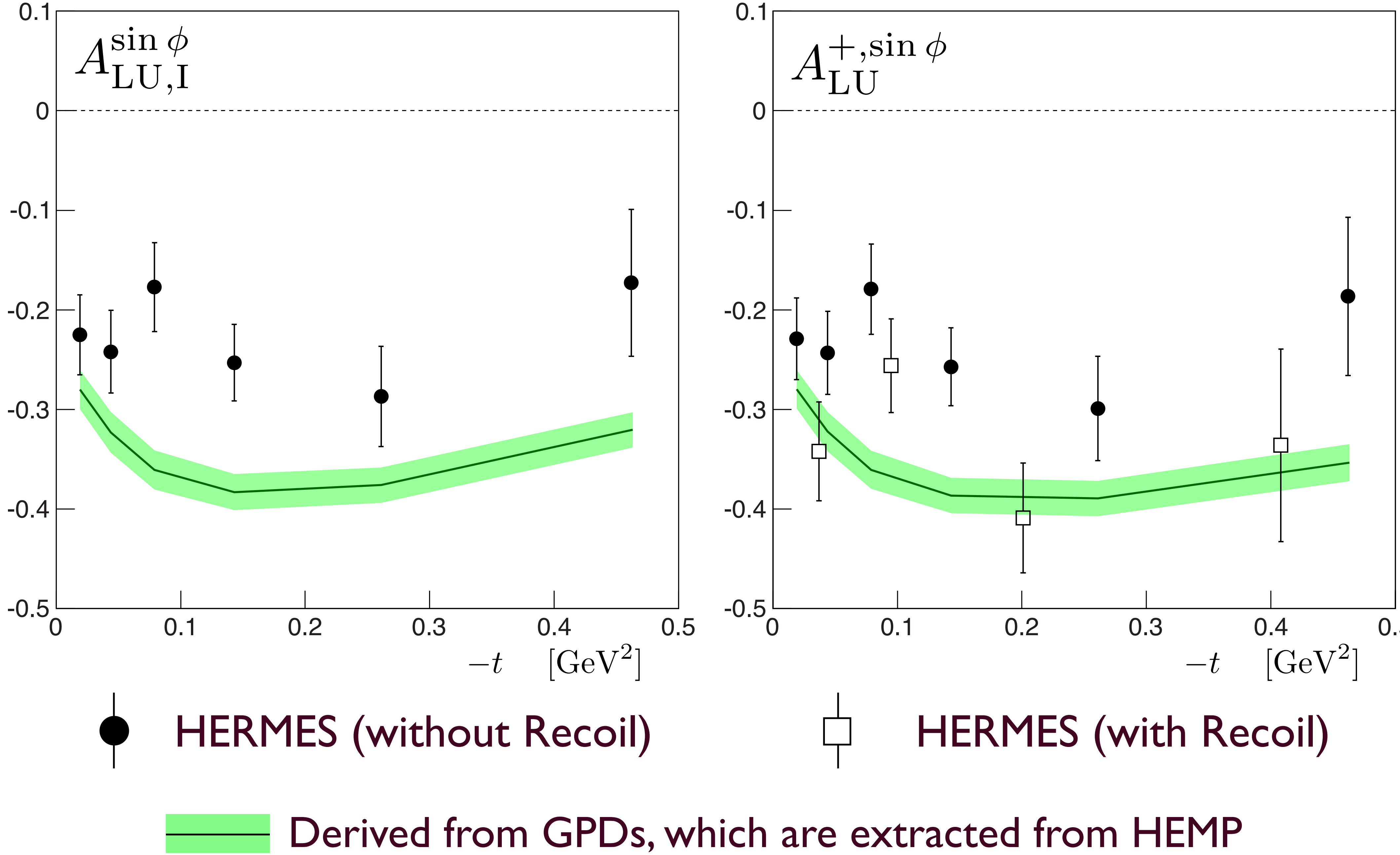

Recoil data leads to a significantly better overlap with HEMP data

Beam-spin asymmetries ep→eγNπ

Besides a better understanding of the unresolved sample, associated DVCS in principle also allows further access to GPDs.

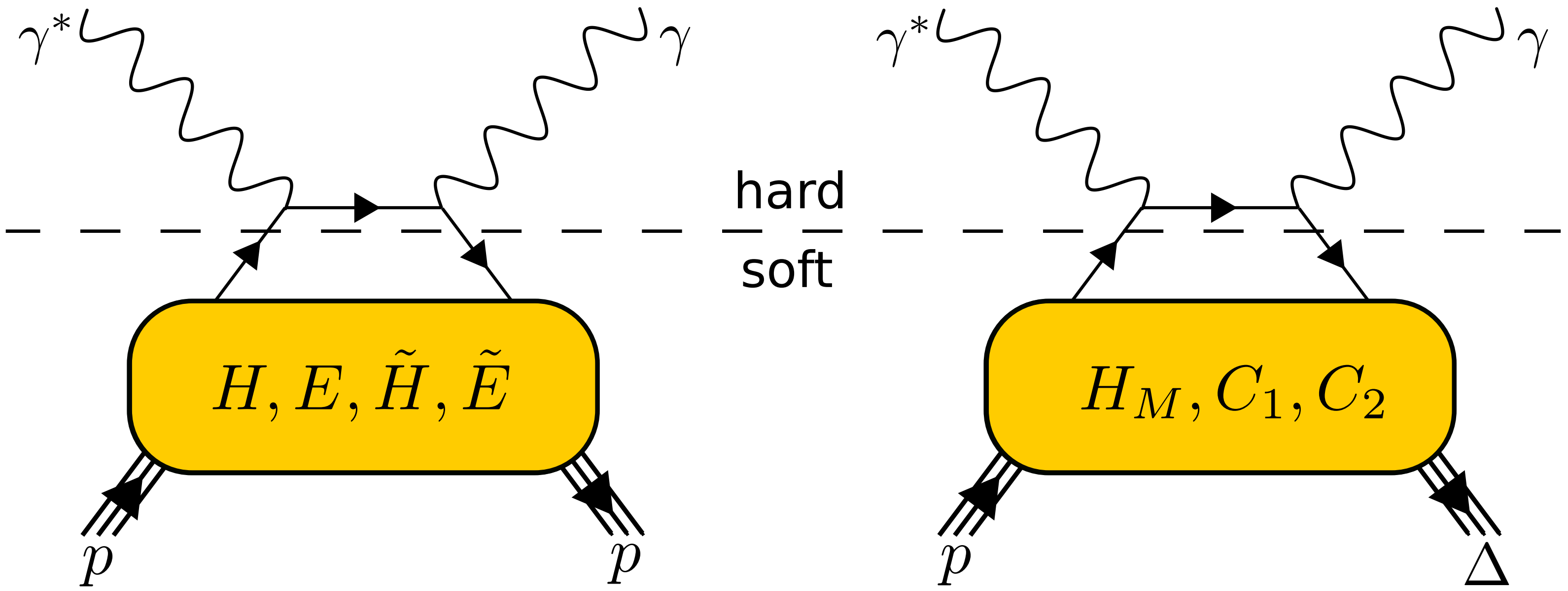

In the large N_c-limit the remaining N→Δ GPDs can be related to the N→N isovector GPDs:

$$H_M(x,\xi,t) = \frac{2}{\sqrt{3}}\left[E^u(x,\xi,t) - E^d(x,\xi,t)\right],$$

$$C_1(x,\xi,t) = \sqrt{3}\left[\tilde{H}^u(x,\xi,t) - \tilde{H}^d(x,\xi,t)\right],$$

$$C_2(x,\xi,t) = \frac{\sqrt{3}}{4}\left[\tilde{E}^u(x,\xi,t) - \tilde{E}^d(x,\xi,t)\right]$$

Selection of associated events

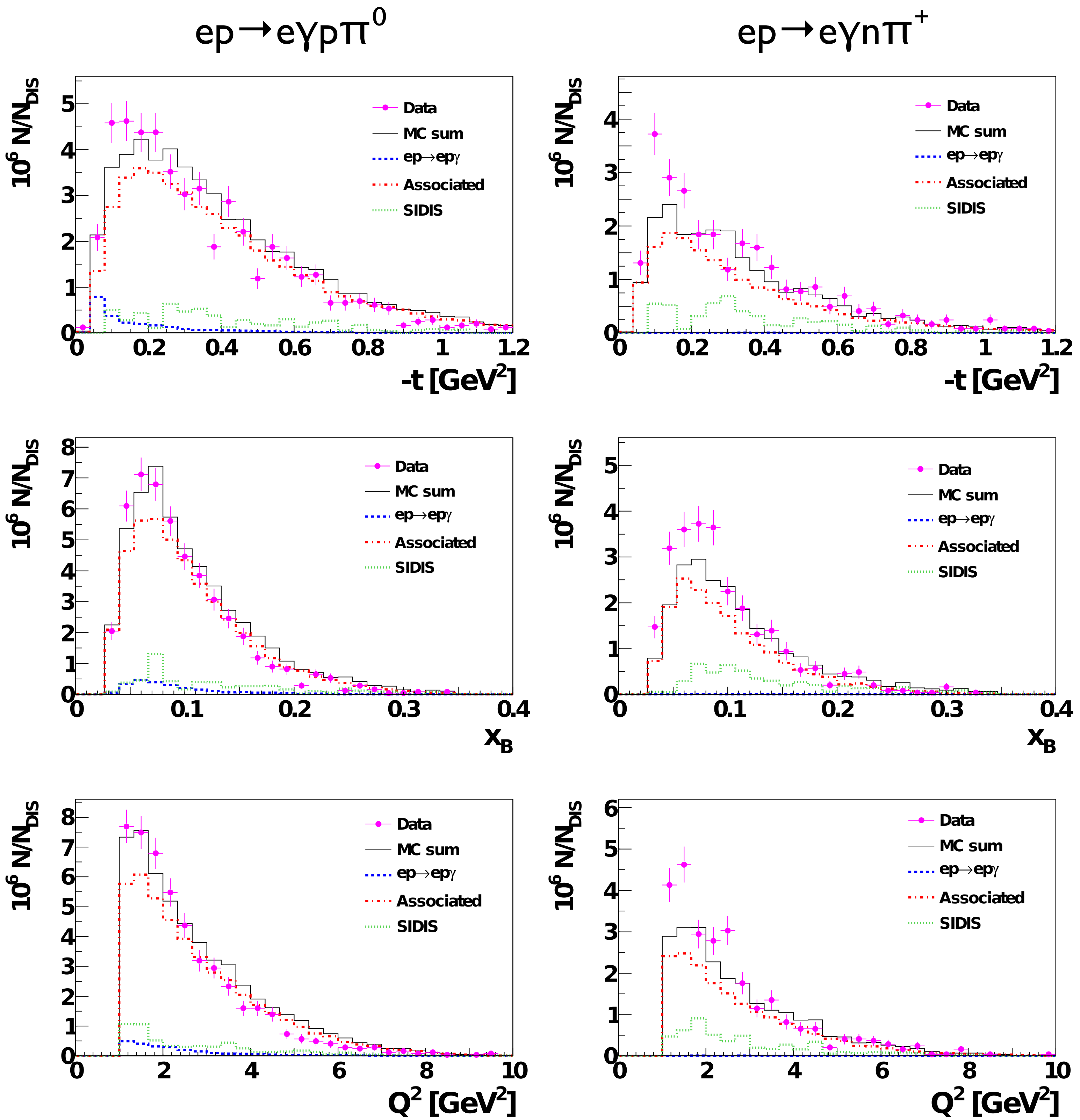

Uncharged particle remains undetected

Kinematic fitting in case of ep→eγNπ hypothesis therefore not as strong

Additional selection criteria:

- Recoil PID information
- Lower-cut on ep→eγp hypothesis

Beam-spin asymmetries $ep \rightarrow e\gamma p\pi^0$

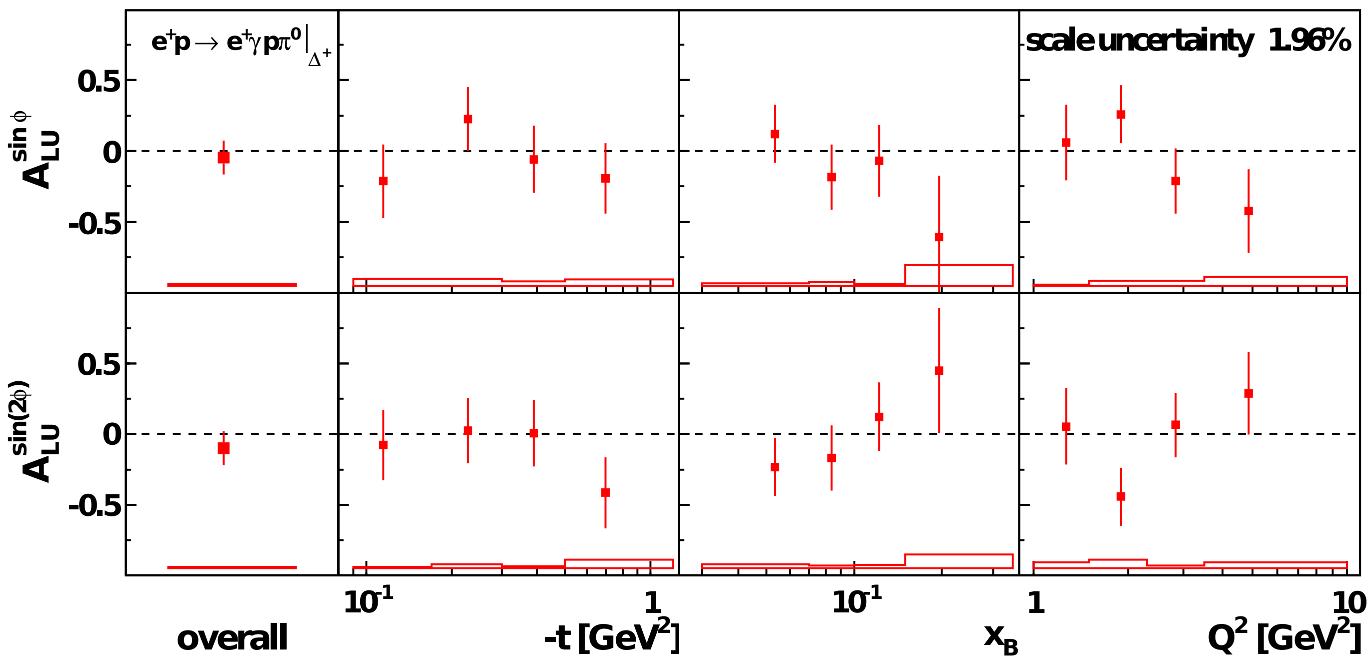

A. Airapetian et al, arXiv:1310.5081; JHEP 14 (in press)

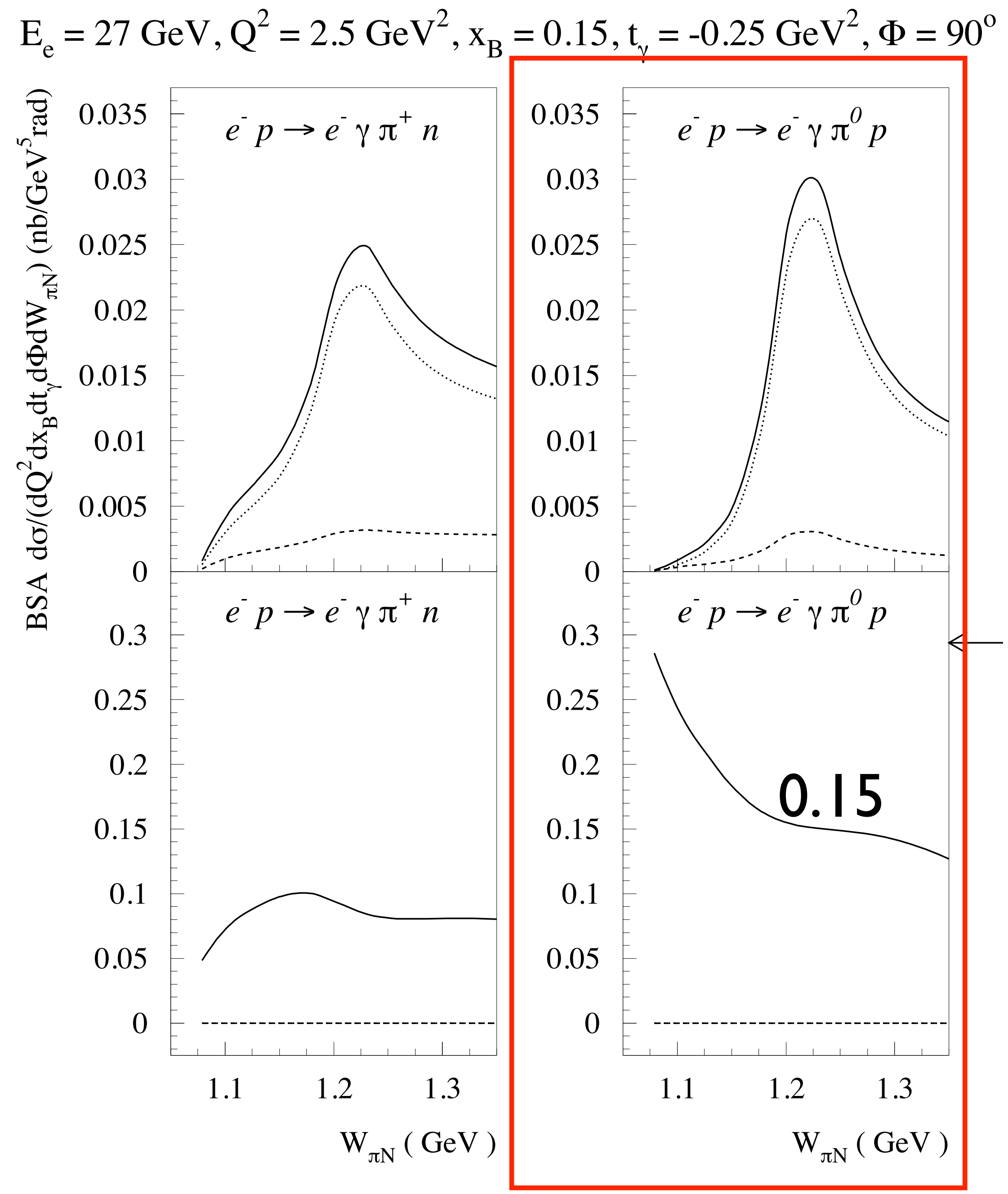

P.A. M. Guichon, L Mossé, M. Vanderhaeghen, Phys. Rev. D 68 (2003

Shown amplitudes are corrected for background (only overall fractions are listed here):

Associated DVCS/BH ($ep \rightarrow e\gamma p\pi^0$)	85 ± 1
Elastic DVCS/BH ($ep \rightarrow e\gamma p$)	4.6 ± 0.1
SIDIS ($ep \rightarrow eX\pi^0$)	11 ± 1

Beam-spin asymmetries $ep \to e\gamma n\pi^+$

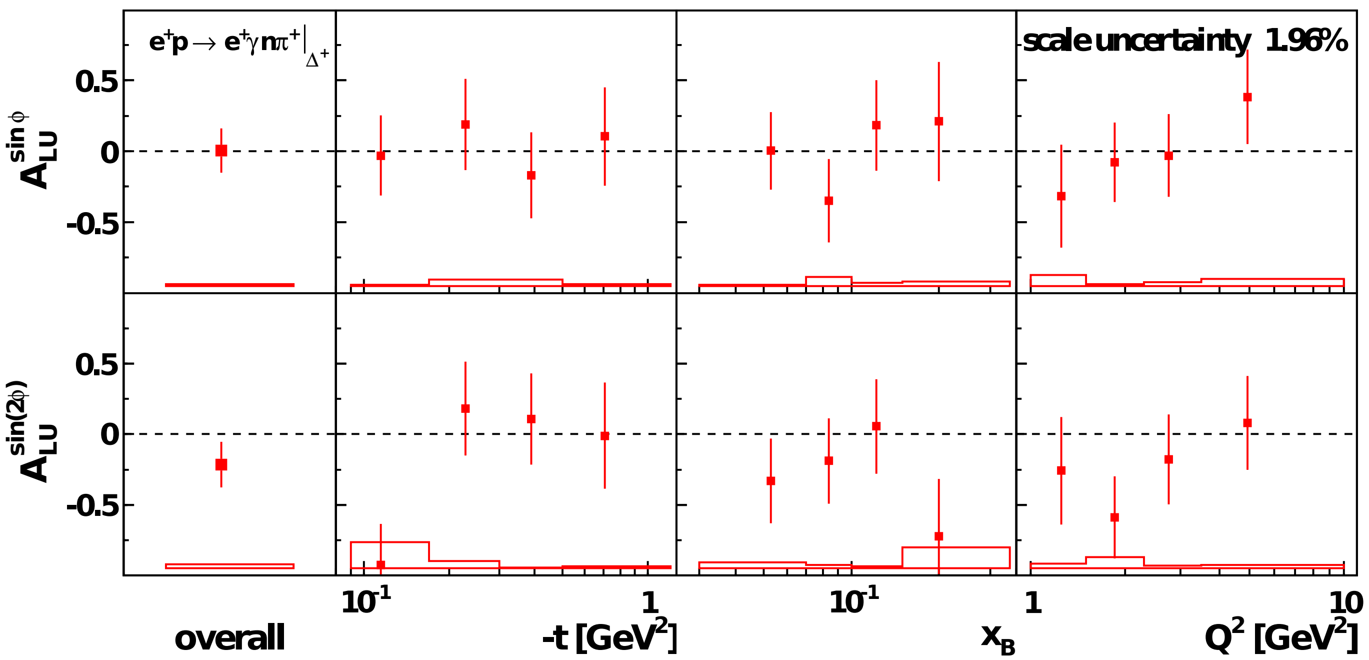

A. Airapetian et al, arXiv:1310.5081; JHEP 14 (in press)

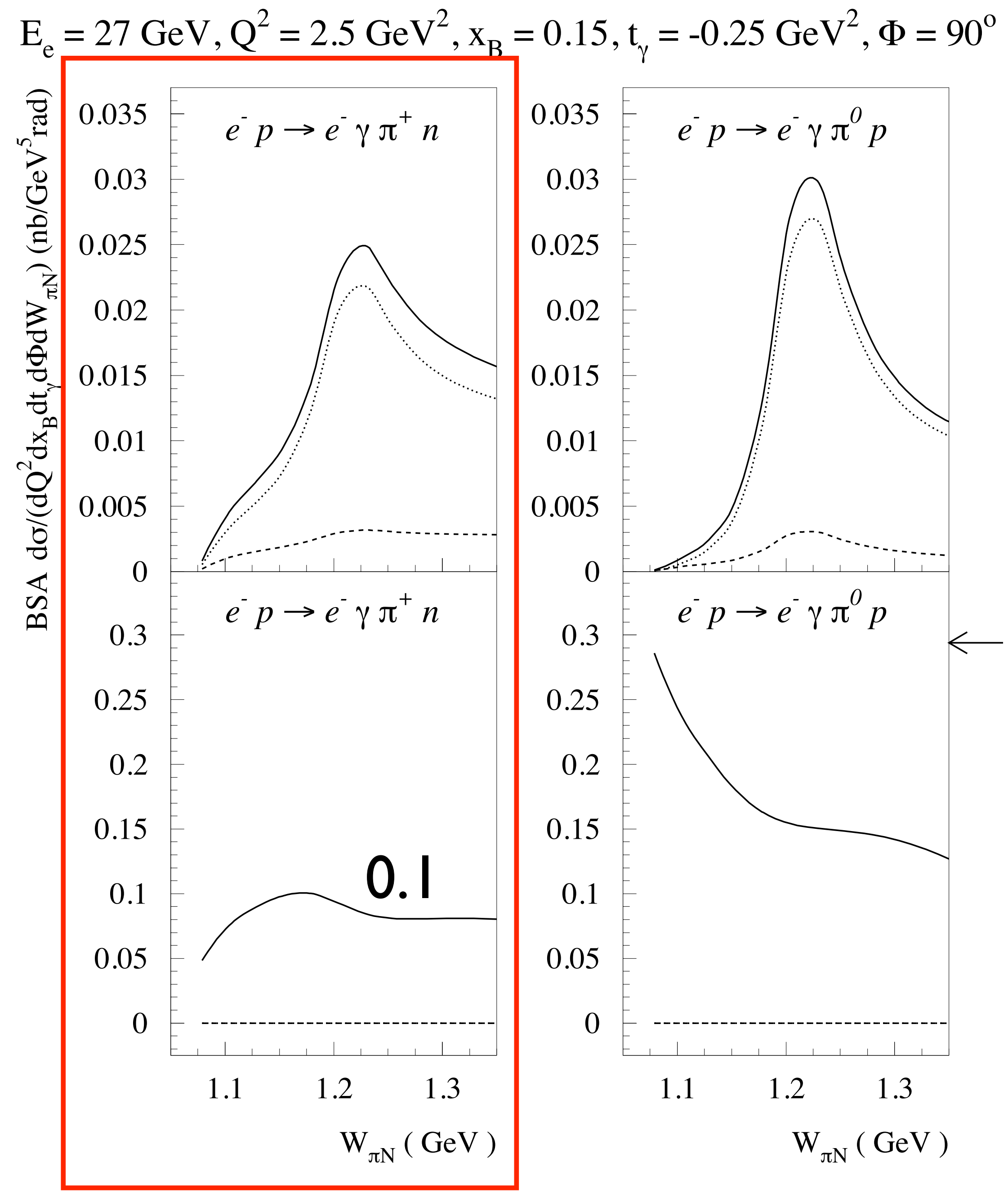

P.A. M. Guichon, L Mossé, M. Vanderhaeghen, Phys. Rev. D 68

Shown amplitudes are corrected for background (only overall fractions are listed here):

Associated DVCS/BH ($ep \to e\gamma n\pi^+$)	77 ± 2
Elastic DVCS/BH ($ep \to e\gamma p$)	0.2 ± 0.1
SIDIS ($ep \to eX\pi^0$)	23 ± 3

HERMES DVCS Summary

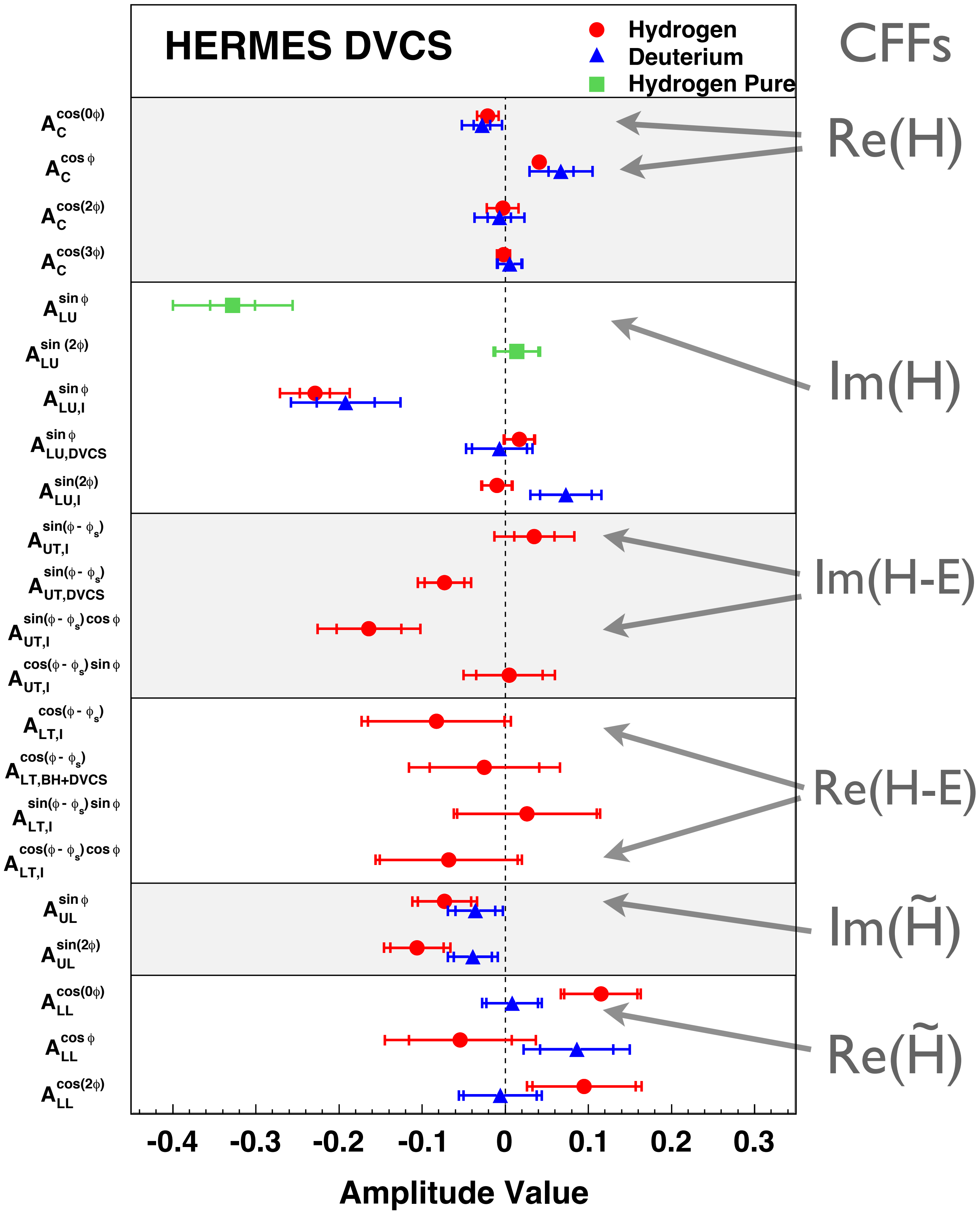

- The HERMES Recoil detector allows complete event reconstruction for $ep\rightarrow e\gamma p$ and reduces the resonant background to a negligible level
- First measurement of asymmetry amplitudes in associated DVCS ($ep\rightarrow e\gamma\pi N$)

A. Airapetian et al, JHEP 06 (2008) 066,
Nucl. Phys. B 829 (2010) 1-27, JHEP 06 (2010) 019,
Nucl. Phys. B 842 (2011) 265-298, JHEP 07 (2012) 032,
Phys. Lett. B 704 (2011) 15-23, JHEP 10 (2012) 042,
arXiv:1310.5081; JHEP 14 (in press),
JINST 8 P05012 (2013)

Backup

Recoil magnet

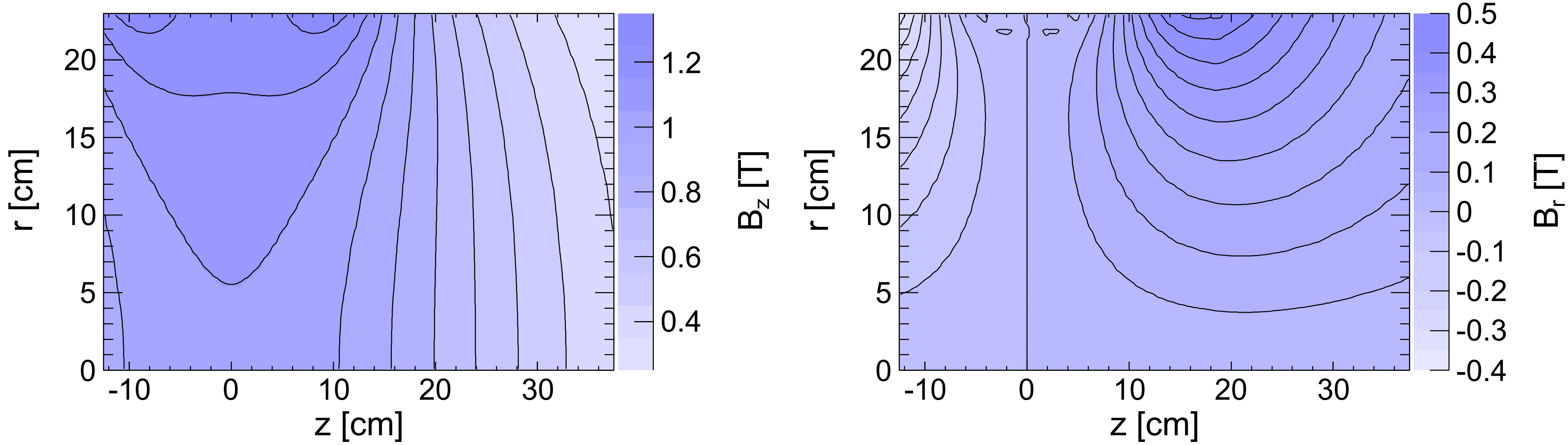

NbTi-wires with 0.85 mm diameter mounted on copper rings

166 A operating current → 1 T at center

SSD (silicon strip detector)

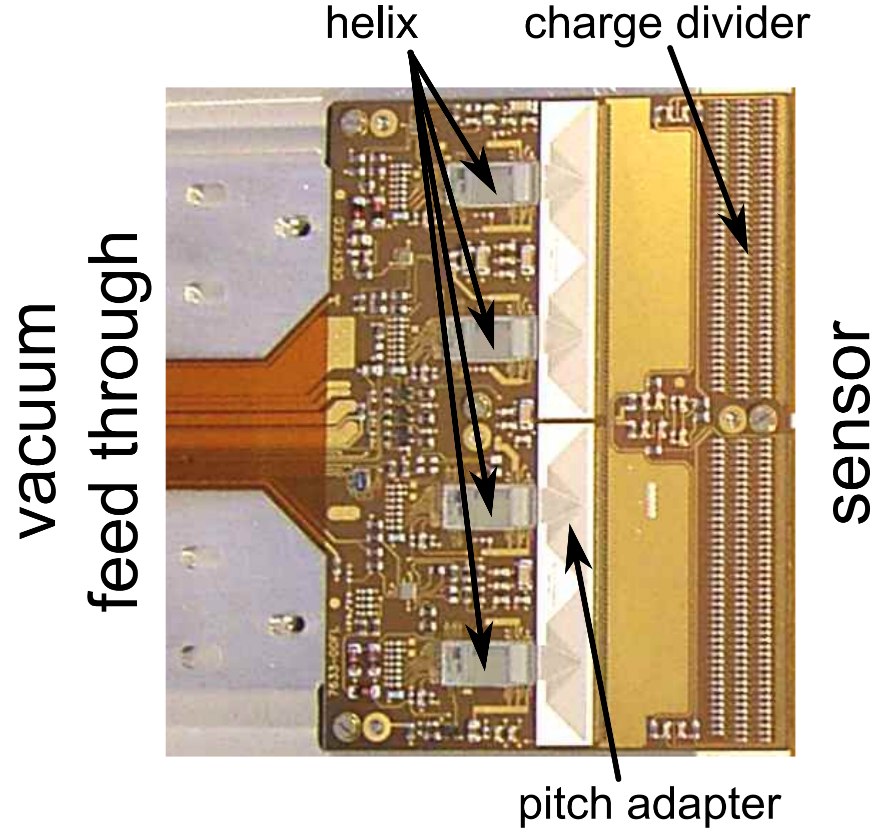

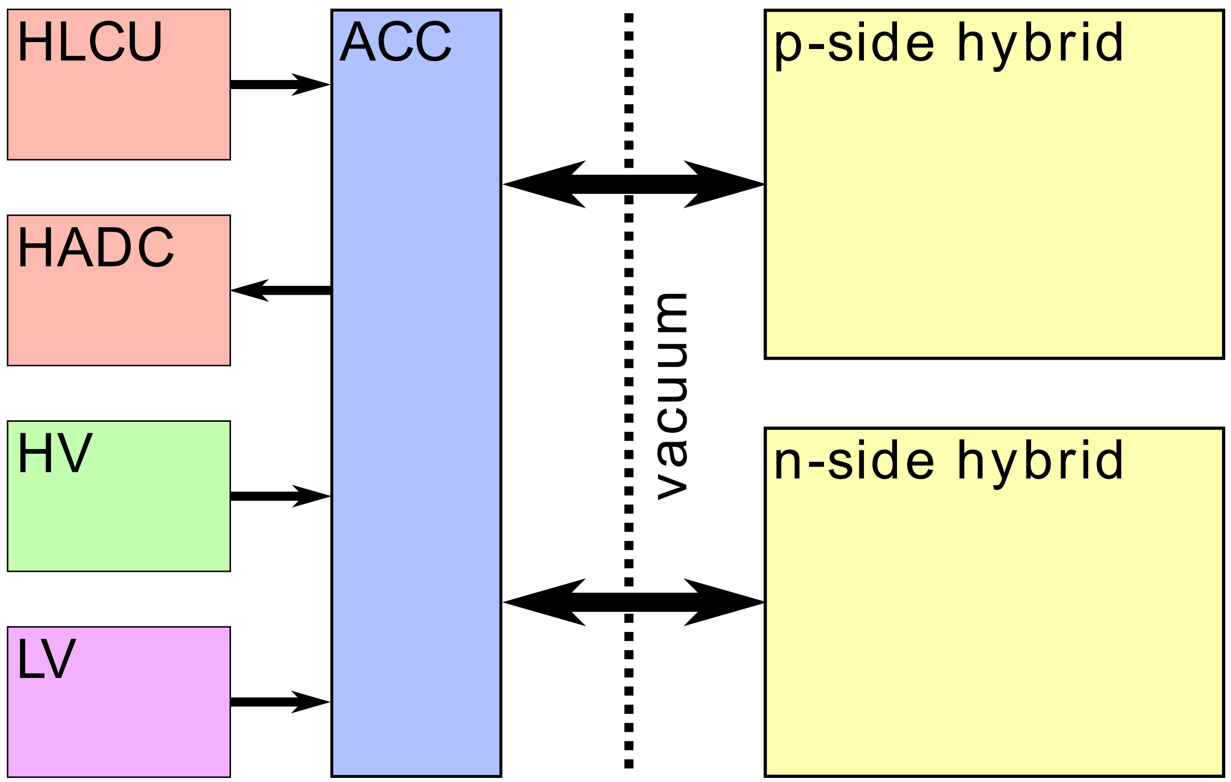

5.8 cm away from lepton beam, 1.5 cm gap

sensor thickness 295 um - 315 um

thickness of target cell 75 um

SFT (scintillating fibre tracker)

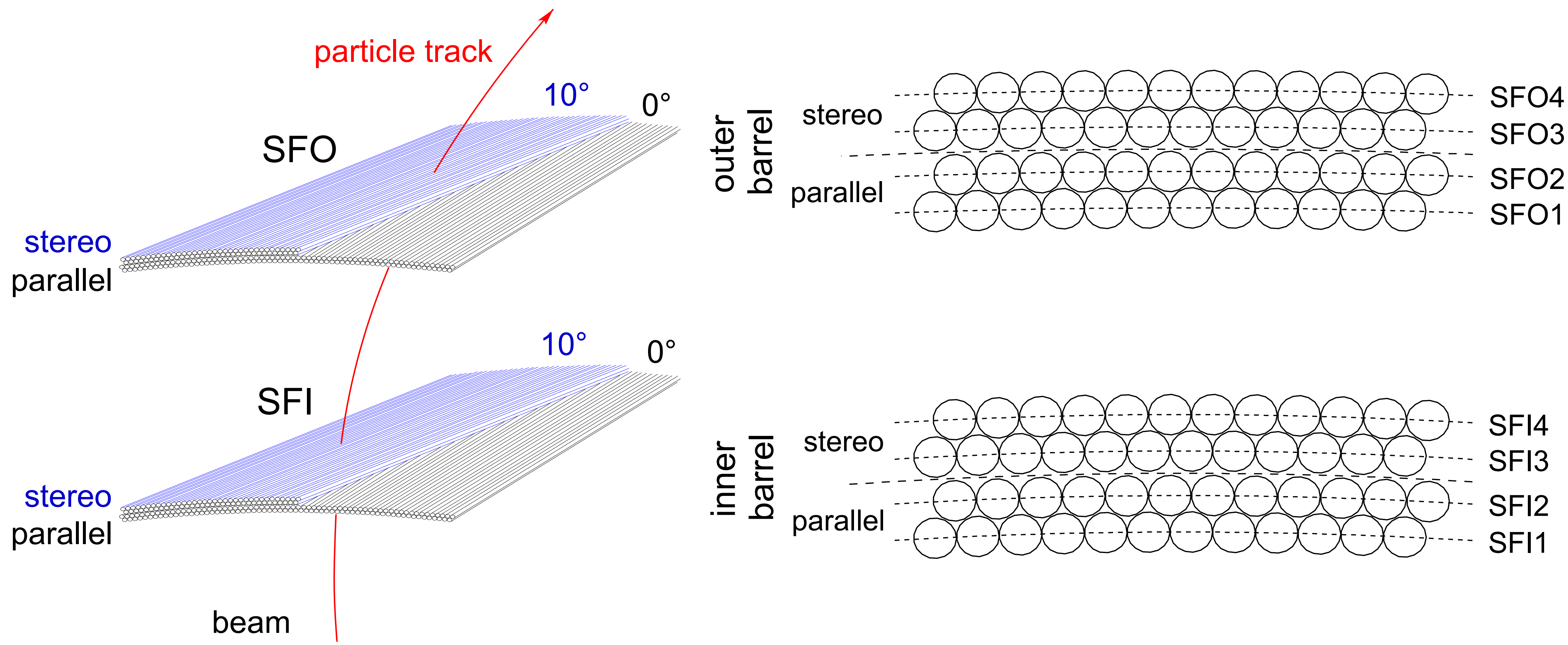

11.5 cm (18.5 cm) inner (outer) radius

1318+1320 (2198+2180) fibres with a diameter of 1 mm each

readout by 64-channel Hamamatsu H7546B MAPMTs

Recoil tracking

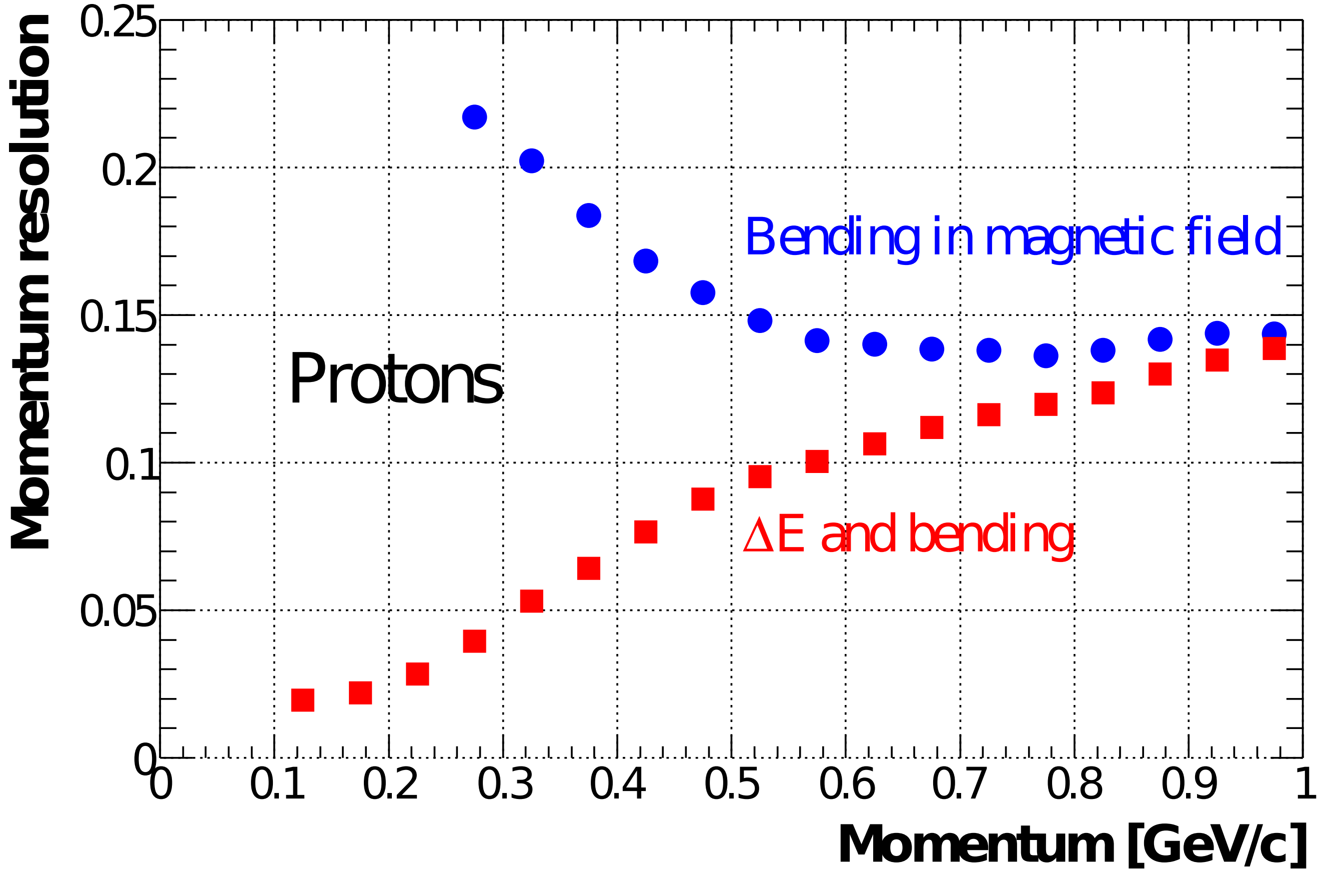

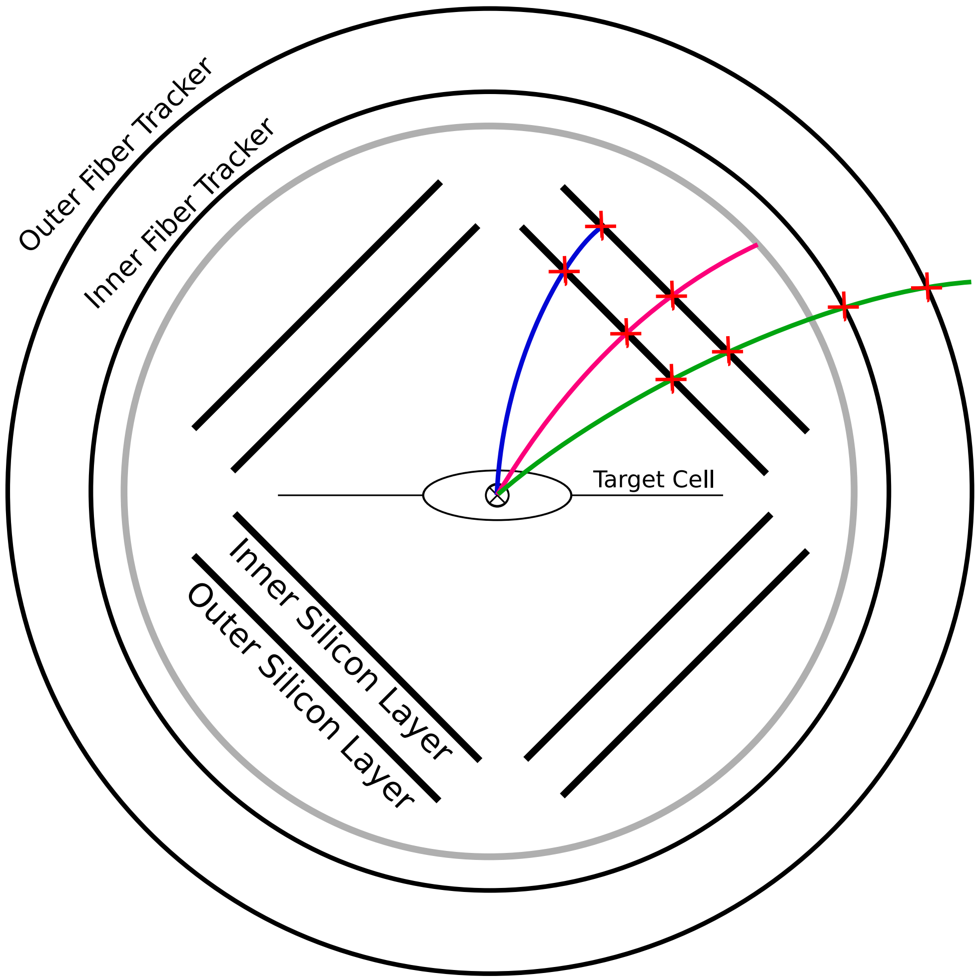

taking energy loss into account improves momentum resolution for low p

azimuthal-angle resolution: 4 mrad, polar-angle resolution: 10 mrad (for p>0.5 GeV)

Recoil PID

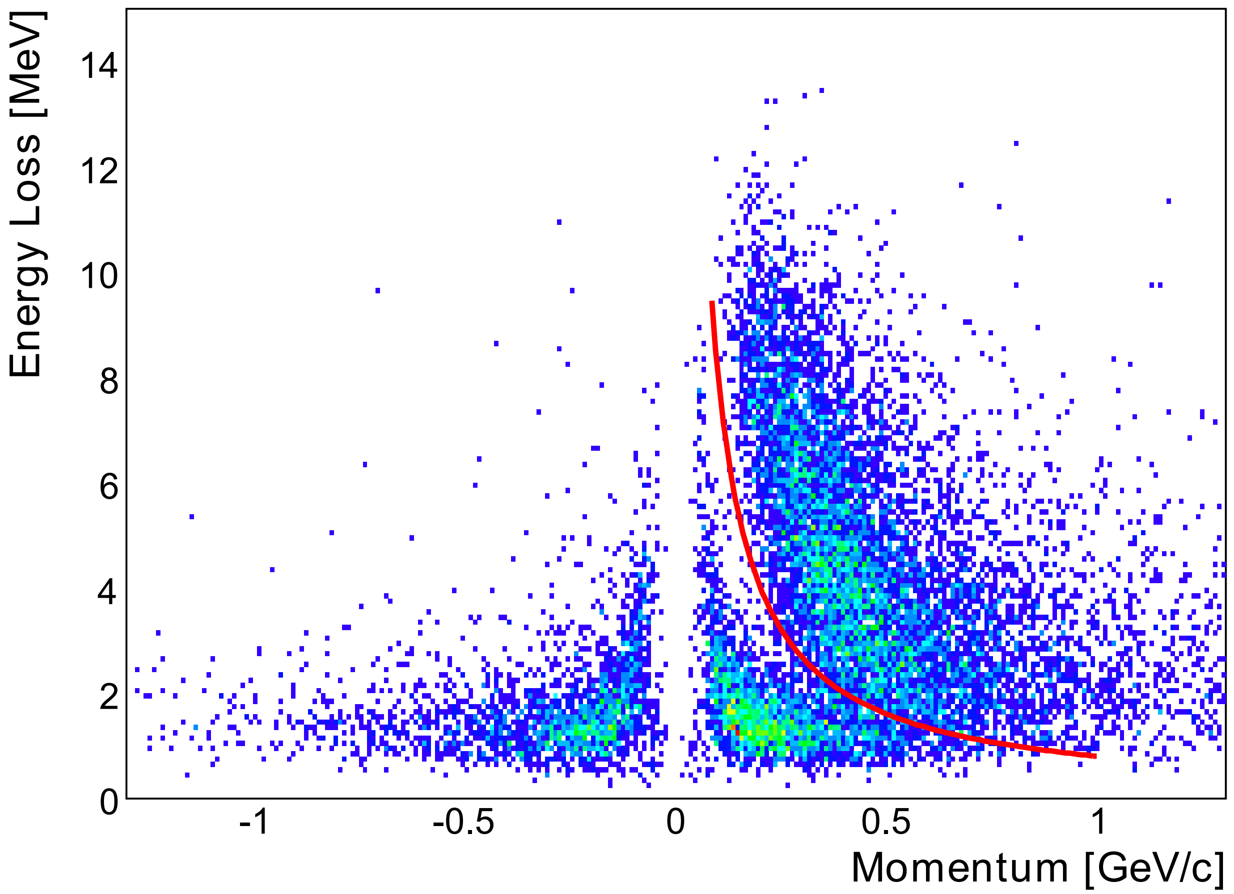

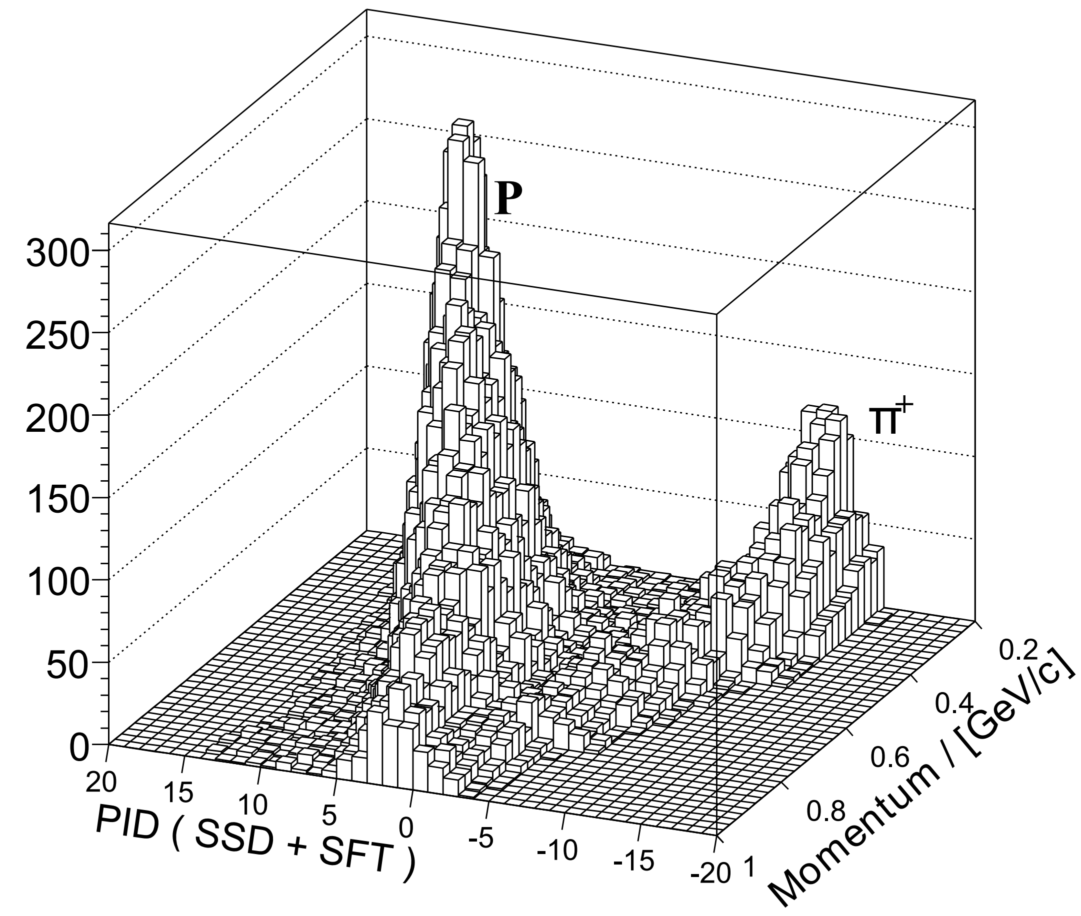

discrimination between protons and positively charged pions

parent distributions were crucial and determined experimentally

Kinematic fitting for ep→eγpπ^0

ep→eγpπ^0 ep→eγp SIDIS

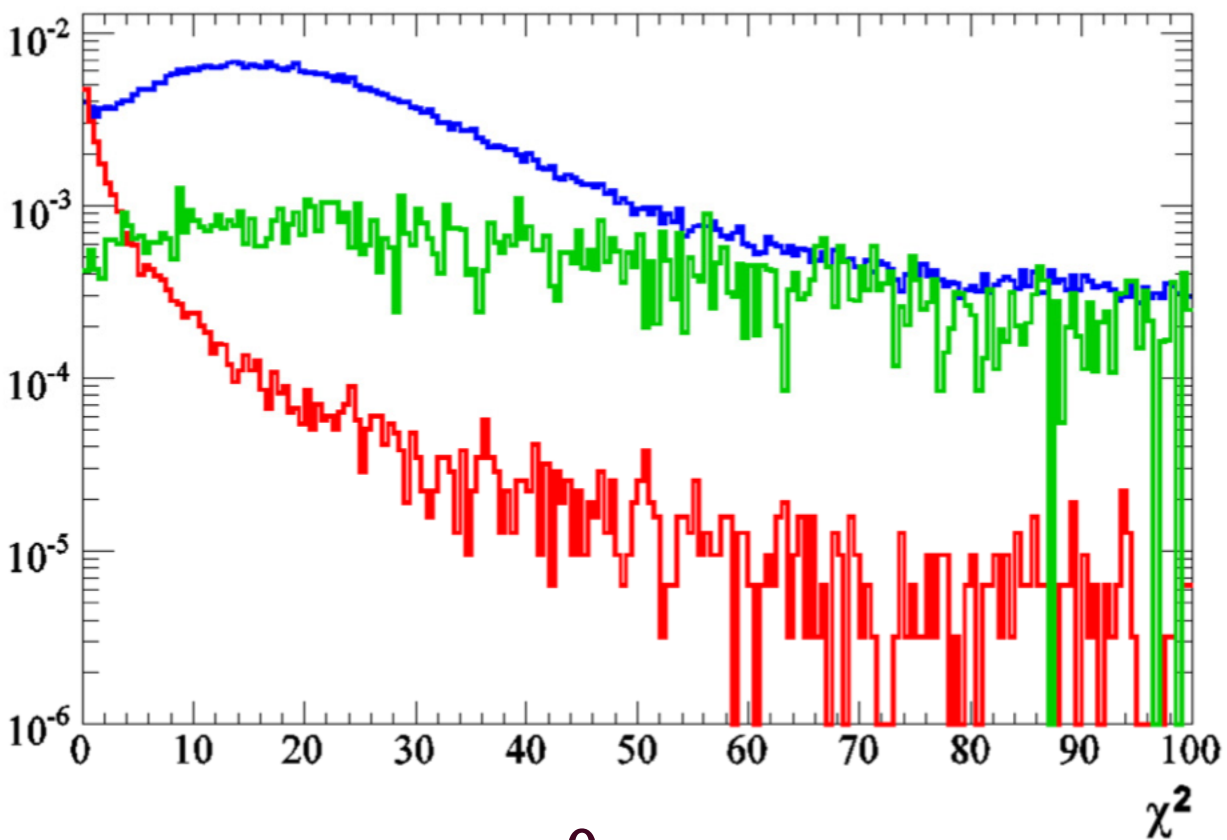

ep→eγpπ^0 hypothesis

$\chi^2_{ep\to e\gamma p\pi^0} < 4.6$

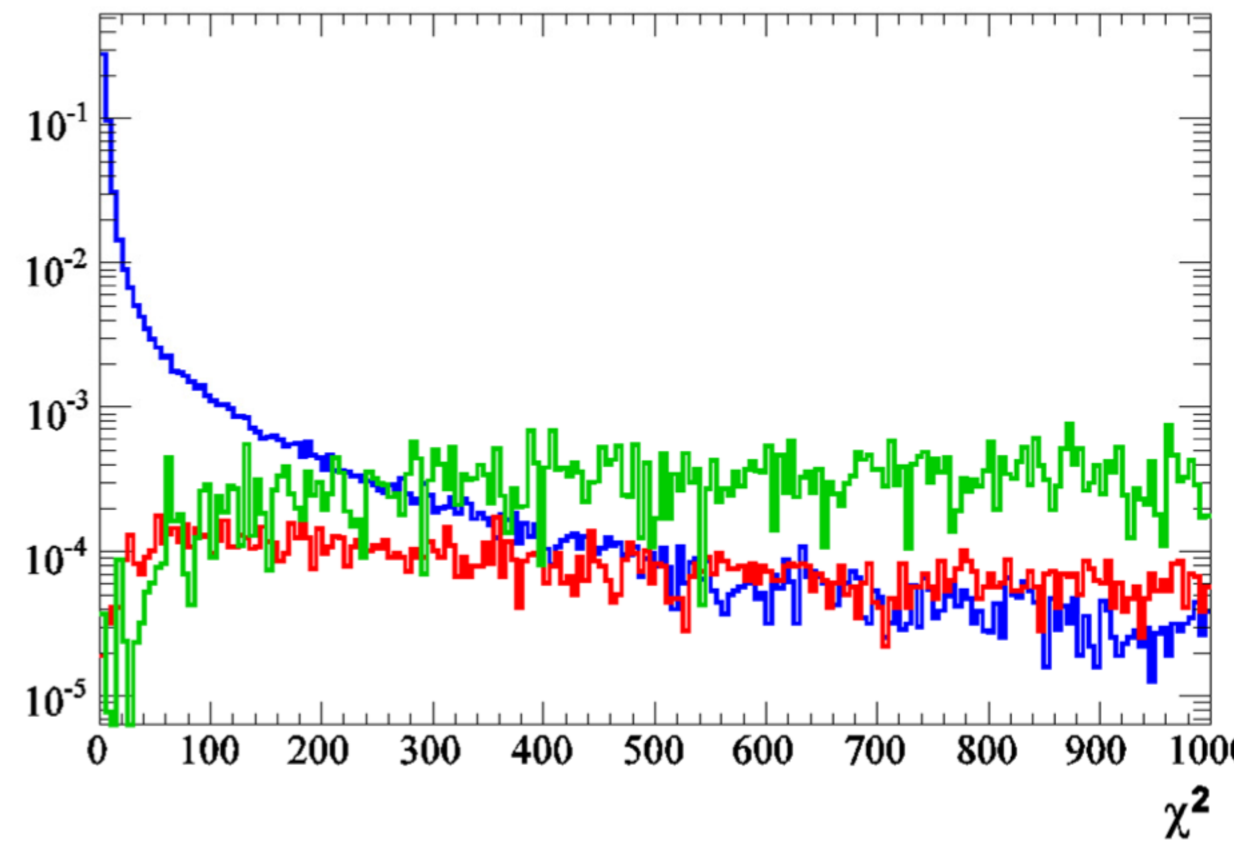

ep→eγp hypothesis

$\chi^2_{ep\to e\gamma p} > 50$

Using powerful kinematic fitting of ep→eγp hypothesis
is crucial for the ep→eγNπ analysis